Cardiac Regenerative Medicine

Shinsuke Yuasa, MD*,**; Keiichi Fukuda, MD*

Severe heart failure is associated with damage to the myocardium that is irreversible with current medical therapies. Recent experimental and clinical studies, however, have opened the possibility of solving many of the associated problems, making this an exciting and tangible goal. There are many potential cell sources for regenerative cardiac medicine, including bone marrow stem cells, endothelial progenitor cells, skeletal myocytes, adult cardiac stem cells, and embryonic stem (ES) cells. Although ES cells are highly proliferative and suitable for mass production, they are not autologous, and an efficient protocol is yet to be established to ensure selective cardiomyocyte induction. Recent studies have successfully established inducible pluripotent stem (iPS) cells from mouse and human fibroblasts by the gene transfer of 4 transcription factors that are strongly expressed in ES cells: *Oct3/4*, *Sox2*, *Klf4* and *c-Myc*. iPS cells can differentiate into all 3 germ layer-derived cells and are syngeneic, indicating that they can become an ideal cell source for regenerative medicine. Despite these successes, the accumulating evidence from fields as diverse as developmental biology, stem cell biology and tissue engineering must be integrated to achieve the full potential of cardiac regenerative medicine.   (*Circ J* 2008; **Suppl A:** A-49–A-55)

Key Words: Cardiomyocyte; Cell differentiation; Cell transplantation; Stem cell; Tissue engineering

Heart failure is associated with decreased blood supply to tissues throughout the body[1] and in severe heart failure this can lead to markedly reduced cardiac systolic function. One exciting potential therapeutic option to improve cardiac function and mortality is the transplantation of healthy regenerative cardiomyocytes into the injured heart. Many potential cell sources can be utilized in regenerative cardiac medicine, including bone marrow (BM) stem cells, endothelial progenitor cells, skeletal myocytes, adult cardiac stem cells, and embryonic stem (ES) cells. BM mesenchymal stem cells (MSC) have been central to the development of cardiac regenerative medicine since we first reported that BM cells could differentiate into cardiac myocytes in 1999[2] Hematopoietic stem cells (HSC), endothelial progenitor cells, ES cells, cardiac tissue stem cells, and adipose tissue stem cells have also been found to undergo myocardial differentiation, and it is possible that additional cell types may have cardiac differentiation abilities as well[3–6] To date, a number of clinical trials have been performed using BM mononuclear cells, circulating endothelial progenitor cells, skeletal myoblasts, and MSC[7–9]; however, the results of these trials have been unsatisfactory because of the poor efficiency of differentiation into cardiomyocytes. In addition, the mechanism by which stem cell transplantation improves cardiac function remains obscure. Therefore, our main task involves refining methods that will enable the selective differentiation of stem cells into cardiomyocytes, optimizing the route of administration of stem cells, and specifically inducing heart tissue regeneration. This review will focus on the recent advances in cardiac regenerative medicine.

Generation of Inducible Pluripotent Stem (iPS) Cells

Compared with adult stem cells, ES cells are derived from the blastocyst embryo, have a strong proliferative ability and promising differentiation capability. However, ES cells are allogeneic, and strong autologous stem cells are better suited to tailoring cardiac regenerative medicine practices to individual patients. Based on this ideal, the most notable event in recent years is the successful generation of iPS cells. Murine iPS cells were generated from adult mouse fibroblasts by ectopic expression of 4 transcription factors: *Oct3/4*, *Sox2*, *c-Myc*, and *Klf4*[10] The morphology, growth properties and pluripotency of these iPS cells are very similar to those of mouse ES cells. Moreover, the germline competency of murine iPS cells was demonstrated by using the *cis*-element of Nanog as a selection marker[11] *c-Myc* is a known oncogene, but a recent study demonstrated that this gene is not required for the generation of iPS cells and that iPS cells without *c-Myc* did not develop tumors[12] Human iPS cells have also been created from human adult somatic cells by gene transfer of the same 4 transcription factors: *Oct3/4*, *Sox2*, *c-Myc*, and *Klf4*, without selection[13–15] Successful reprogramming of differentiated human somatic cells into a pluripotent state would allow the creation of stem cells specific to individual patients. The accumulating knowledge regarding ES cell differentiation is advancing the development of differentiation protocols[16,17] As the stem cell characteristics of iPS cells resembles those of ES cells, it is likely that the cell differentiation methods of iPS cells will also resemble those of ES cells. Therefore, it is important that the results of ES cell-derived cardiomyocyte differentiation strategies are taken into account, so that the clinical application of iPS cells can occur in the near future.

ES Cells

The first mouse ES cell line was established by Evans and Kaufman in 1981, and ES cells were initially used as a model for the analysis of embryonic development and for generating genetically modified mice.[18-20] In the mid-1990s, ES cell research slowly moved to stem cell-based research into cell transplantation therapy using in vivo animal models.[21,22] In 1998, Thomson et al first reported the establishment of human ES cells[23] and although ethical issues surrounding their use still remain, they quickly attracted significant attention as a source for regeneration therapy. Researchers were interested in the proliferative and differentiation powers of ES cells, but were also aware that the immunological problems of allogeneic ES cells needed to be resolved before these cells could be used in a clinical setting. In 2001, Wakayama et al established murine ES cells by applying nuclear transfer techniques to nuclei derived from somatic cells.[24] Their findings strongly suggested that an individual's own ES cells could be generated by using somatic cells, thereby obviating immune rejection.[25,26] However, nuclear transfer techniques are technically difficult, so it was important to develop simpler methods for widespread use.

The in vitro differentiation of cardiomyocytes from mouse ES cells was first reported in 1985.[27] In 1996, Klug et al described the stable transfection of ES cells with a cDNA encoding aminoglycoside phosphotransferase under the control of the α-cardiac myosin heavy chain promoter and these cells differentiated into a relatively pure population of cardiomyocytes in the presence of suitable antibiotics.[21] That study provided the impetus that encouraged the use of ES cells in the clinical setting. The development of methods for differentiating ES cells into cardiomyocytes more selectively and efficiently using a variety of factors progressed steadily from the late 1990s.[23,28-34] The differentiation of ES cells into any cell lineage partly mimics the physiological regulatory mechanisms that occur during normal early development. Although several signaling protein families, including BMPs, Wnts, Notch, and FGFs, are involved in the development of the heart, limited evidence is available about the exact signals that mediate the differentiation of ES cells into cardiomyocytes. In mouse embryos, cardiac progenitor cells appear around embryonic stage 7.0 (E7.0) and the cardiac crescent is formed by E7.5, indicating that the growth factors expressed in these regions and around the cardiac crescent may have an important role in cardiomyocyte induction.[35,36] BMPs are expressed in the lateral plate mesoderm including the anterior lateral plate, and gene targeting of *BMP-2* causes severe heart deformity in early-stage embryos.[37] Application of BMP-2-soaked beads in vivo has also been used to induce the ectopic expression of cardiac transcription factors, and the administration of soluble BMP-2 or BMP-4 to explant cultures induces cardiac differentiation in premature non-cardiogenic mesoderm.[38] These findings strongly suggest a critical role for BMPs in the induction of cardiomyocytes. In contrast, both BMP-2 and BMP-4 inhibit cardiomyogenesis before and during the early stages of gastrulation.[39] Additionally, we have observed that simple stimulation with BMP-2/BMP-4 does not augment or suppress cardiomyocyte induction from ES cells. We hypothesized that BMP antagonists may also be involved in cardiomyocyte induction and found that the BMP antagonist, Noggin, was transiently but strongly expressed in the heart-forming area. We speculated

that the context-dependent differential action of BMPs in cardiomyocyte induction might be explained by the local action of Noggin and other BMP inhibitors, and accordingly developed a protocol to induce cardiomyocyte differentiation from ES cells by transient Noggin addition. Expression of Noggin prior to the embryoid body (EB) formation stage mimicked the transient and strong expression of Noggin during the early gastrulation stage. In particular, expression of Noggin at 3 days and 0 days before EB formation led to a marked increase in the incidence of beating EBs 10 days after EB formation.[40]

Wnt signals also play major roles in cell adhesion, morphology, proliferation, migration, and structural remodeling during the developmental process.[41-44] The major components of this network are the Wnt ligands, which bind to Frizzled receptors at the cell surface. The Wnt ligands comprise at least 17 members, with some activating the canonical Wnt/β-catenin pathway and others activating the non-canonical pathway. Cytosolic β-catenin associates with cadherins on the intracellular side of the plasma membrane to promote cell adhesion, and with the actin microfilament network to control cell shape. Activation of Wnt signaling downregulates the intracellular degradation of β-catenin, thereby allowing it to translocate to the nucleus and activate other transcription factors in conjunction with its co-transcription factors, the LEFs/TCFs. The non-canonical Wnt pathway has no role in regulating β-catenin degradation, but can activate JNK and other signaling pathways. In past studies, Wnt signaling had been implicated as an inhibitor of cardiomyocyte induction.[45] Studies have shown that Wnt inhibitors, Crescent and Dkk-1, are expressed in the anterior endoderm during gastrulation and could induce the formation of beating heart muscle, and that ectopic Wnt signals could repress heart formation from the anterior mesoderm in vitro and in vivo.[46-48] In addition, the forced expression of either Wnt3A or Wnt8 promotes the development of primitive erythrocytes from the precardiac region. These findings indicate that inhibition of Wnt signaling by the diffusion of Dkk-1 and Crescent from the anterior endoderm promote heart formation in the anterior lateral mesoderm.

In contrast, the mesodermal marker, Brachyury(T), is a target of Wnt3, one of the canonical Wnt signaling ligands.[49] It was therefore expected that canonical Wnt signaling played a role in cardiac development. Recent reports have demonstrated that Wnt members play positive roles in cardiomyocyte differentiation in vitro and in vivo.[45] In particular, Wnt11 is expressed in the early mesoderm in a pattern that overlaps with the precardiac regions.[50] In addition, exogenous Wnt11 can promote cardiac differentiation in vitro and in vivo through the independent β-catenin pathway, but is dependent on protein kinase C and JNK.[50,51] The involvement of Wnt family members and β-catenin in mammalian cardiac myogenesis was examined using a pluripotent mouse embryonic carcinoma cell line (P19CL6), which can be induced to differentiate into cardiomyocytes by 1% DMSO.[52] The administration of DMSO induced Wnt3A and Wnt8A, which in turn activated Wnt/β-catenin signaling and thereby induced cardiac myogenesis in the P19CL6 cells. These findings indicated that Wnt/β-catenin signaling is activated at the inception of mammalian cardiac myogenesis in this pluripotent model system. Accumulating evidence has also shown that the Wnt pathway plays a crucial role in cardiomyocyte induction, although temporal and spatial regulation seems to be critical for cardiac develop-

ment[53-56]

There is no single growth factor that acts constantly throughout the entire process of organ induction during the development of multiple organ systems; it is the time- and context-dependent expression of multiple factors that is critical for proper development. A single factor such as BMP, Wnt, Notch, or Hedgehog can exert opposite actions during different developmental processes. The use of growth factor combinations in their in vivo context will facilitate the specific differentiation of cardiomyocytes from ES cells in the near future. In 2001, it was reported that human ES cells, like mouse ES cells, could differentiate into cardiomyocytes with cardiac-specific structural and functional properties[57] The same group recently revealed that transplanted human ES cell-derived cardiomyocytes can act as a pacemaker in porcine ventricles in which a complete atrioventricular block was artificially generated, and improve cardiac performance in the infarcted rat heart[58,59] This study demonstrated that human ES cell-derived cardiomyocytes could make a successful electrical connection with recipient cardiomyocytes in large animals. Studies such as this one have demonstrated that research into ES cells as a source for regenerative medicine has progressed rapidly in recent years, and this also applies to human iPS cells, making feasible the clinical application of these cells as a source of cardiomyocytes in transplantation therapy.

BM Stem Cells

In 1966, MSC were initially identified in BM and were known as bone formation progenitors[60] For some time thereafter, BM-MSCs were believed to differentiate into osteoblasts, chondroblasts, adipocytes, and connective tissues only[61,62] Subsequently, MSCs were reported to comprise approximately 0.001–0.01% of the total nucleated cells in BM, which is far less than that of HSCs[63,64]

BM-MSCs were initially isolated from BM stromal cells by their morphology, proliferative activity and multipotency. Recent studies have demonstrated that BM-MSCs can also differentiate into neurons, skeletal muscle cells and cardiomyocytes, both in vitro and in vivo. Recent advances in fluorescence-activated cell sorting (FACS) techniques have enabled isolation of different cells by cell surface antigen expression and fluorescent dye efflux characteristics[65,66] FACS analysis revealed that the HSC population in mice consists of a CD34⁻ c-kit⁺ Sca-1⁺ Lin⁻ tip-side cell population (SP), in which c-kit is a stem cell factor receptor, Sca-1 is a stem cell antigen specifically expressed in various stem cells in mice only, and Lin is a mixture of antibodies against lineage markers for hematocytes[67] Despite some reports, cell surface markers able to isolate MSCs have yet to be determined. CD29, CD44, CD105, and murine Sca-1 are widely accepted cell surface markers for MSCs, but the acceptability of other markers differs among researchers[68-70]

In 1999, we induced functional cardiomyocyte differentiation from mouse MSCs with 5-azacytidine, which demethylates methyl-cytosine[2] At the time, this was considered a very surprising phenomenon because BM cells were thought to only differentiate into either blood cell lineages or bone cells. This finding was later pursued using a variety of approaches and BM cells were shown to have the potential to differentiate into a variety of tissues, including cardiomyocytes. In 2001, Beltrami et al observed mitotic cardiomyocytes in human hearts after a myocardial infarction;[71]

however, it was unknown whether mature cardiomyocytes had acquired the ability to proliferate, whether immature cardiomyocytes already residing in the adult heart had differentiated from stem cells into proliferating cardiomyocytes, or whether mature cardiomyocytes had acquired the ability to proliferate by fusing with cells that already had proliferative ability. In 2001, Orlic et al reported that transplanted c-kit⁺ Lin⁻ BM cells could differentiate into cardiomyocytes in peri-infarct tissue after myocardial infarction[72] In 2002, numerous recipient-derived cardiomyocytes were observed in a donor heart following human heart transplantation[73] and in 2003, numerous BM-derived cardiomyocytes were also shown to be present in the recipient heart after BM transplantation[74] Subsequently, many studies examined the differentiation capacity of BM cells, the type of cells that BM cells were able to differentiate into and other possible mechanisms. Wagers et al examined a variety of organs after transplanting single GFP-labeled HSC (c-kit⁺, Lin⁻, Sca-1⁺) into irradiated mice and demonstrated that if HSC trans-differentiation does occur, it is extremely rare[75] Goodell et al transplanted highly enriched HSCs into lethally irradiated mice, and following subsequent ischemia – reperfusion injury, found that HSCs differentiated into cardiomyocytes in the peri-infarct region at a prevalence of 0.02%[66] In 2004, Balsam et al investigated whether c-kit⁺ HSCs in BM are capable of differentiating into cardiomyocytes by directly injecting BM cells into the heart instead of transplanting them after irradiation. The results demonstrated that c-kit⁺ HSCs could not differentiate into cardiomyocytes without the effects of irradiation[76] Murry et al reported similar results[77] During this same period, we also examined the differentiation ability of HSCs using a c-kit⁺ Sca-1⁺ CD34⁻ Lin⁻ side population (CD34⁻KSL-SP) of HSCs[78] When we transplanted whole BM cells, which included both HSCs and MSCs, from GFP-transgenic mice into lethally irradiated mice and induced myocardial infarction, we found very few GFP⁺ (BM-derived) cardiomyocytes. Moreover, we confirmed the presence of predominantly MSC-derived GFP⁺ cardiomyocytes in the group transplanted with cardiomyogenic (CMG) cells. It should be emphasized that the radiation dose must be carefully determined in these BM transplantation experiments, because the radiation sensitivity of MSCs is much higher than that of the hematopoietic cells. We proposed that the differentiation of whole BM cells into populations excluding hematopoietic populations is attributable to MSCs, not HSCs, and that MSCs are mobilized from BM.

A great deal of clinical research has involved harvesting mononuclear cells from BM cells or peripheral blood, and infusing these cells through a catheter into a coronary artery to treat acute myocardial infarction. Strauer et al first reported the transplantation of BM mononuclear cells after a myocardial infarction, which resulted in a slight decrease in the left ventricular end-systolic dimension and infarct region, and an increase in the left ventricular ejection fraction (EF) and regional function[79] The TOPCARE-AMI trial allocated 20 patients with reperfused acute myocardial infarction to receive intracoronary infusion of either BM-derived or circulating blood-derived progenitor cells into the infarct artery and showed a significant increase in the global left ventricular EF and a reduction of end-systolic left ventricular volumes[80] The BOOST trial also transplanted BM mononuclear cells after acute myocardial infarction. In most of the studies, transplantation resulted in similar outcomes[81] The REPAIR-AMI trial, which was the first dou-

ble-blind, placebo-controlled, randomized multicenter study to evaluate the effect of intracoronary transplantation of BMCs on infarct remodeling, also showed that BMCs improved the global left ventricular function in patients with acute myocardial infarction[82] However, despite all these human studies, the mechanistic pathway of BMC differentiation remains unclear and in order for BMC transplantation to become a more powerful tool in the field of regenerative medicine, it must be solved to enable us to improve the effects of BMC transplantation.

Cardiac Stem Cells

Stem cells are present in many adult organs, and contribute to the maintenance of physiological conditions and repair mechanisms in pathological states. However, until recently, the existence of stem cells in the heart was completely unknown. Recent advances in genetic engineering and techniques such as FACS are helping to elucidate the presence and properties of stem cells in the heart.

In 2003, Beltrami et al reported that c-kit+ cells in the adult heart were pluripotent and possessed proliferative ability in vitro[83] These cells were able to differentiate not only into cardiomyocytes but also into smooth muscle cells and endothelial cells. Transplantation of these stem cells into a murine myocardial infarction model confirmed their ability to differentiate into cardiomyocytes in vivo, implying the existence of a tissue repair mechanism by stem cells in the heart. In 2003, Oh et al reported that Sca-1+ cells in the adult mouse heart existed as cardiomyocyte stem cells[84] These cells were capable of differentiating into cardiomyocytes when exposed to 5-azacytidine in vitro, and after being administered to a murine model of myocardial ischemia. In 2004, Messina et al isolated myocardial stem cells capable of proliferating in vitro from the hearts of adult humans and mice[85] After dissociating them by enzyme treatment, they added EGF, bFGF, cardiotrophin-1, and thrombin under low serum conditions, and revealed a cell population that formed spheroids with proliferative and differentiation ability.

We recently reported that rodent cardiac SP cell fractions form clonal spheroids in serum-free medium in the presence of EGF and FGF-2[86] These clones expressed nestin, Musashi-1, MDR-1, and the p75 NGF receptor, all of which are markers of undifferentiated neural precursor cells. Following their initial differentiation, differentiation into neurons, glia, smooth muscle cells, and cardiomyocytes occurred. Neural crest-derived cells have stem cell characteristics, in that they are able to proliferate and differentiate into various types of cells. Some neural crest-derived cells in adults express nestin, Musashi-1 and p75, and can proliferate and differentiate into multiple lineages in vitro. We therefore transplanted rodent cardiosphere-derived cells into chicken embryos and observed their migration to the truncus arteriosus and cardiac outflow tract, where they contributed to the development of dorsal root ganglia, spinal nerves and aortic smooth muscle cells. Lineage studies using double transgenic mice encoding P0-Cre/Floxed-EGFP revealed the presence of undifferentiated and differentiated neural crest-derived cells in the fetal myocardium. Undifferentiated EGFP+ cells expressed GATA4 and nestin, but not actinin, in the fetal or neonatal stage, while the differentiated cells were identified as cardiomyocytes in adults. These results suggest that cardiac neural crest-derived cells migrate into the heart, remain there as dormant multipotent stem cells, and differentiate into cardiomyocytes and typical neural crest-derived cells including neurons, glia, and smooth muscle under the appropriate conditions.

In 2005, Laugwitz et al reported that Isl1 (a LIM homeodomain transcription factor), which is known as a secondary heart field marker, can also be used as a cardiomyocyte progenitor marker in the postnatal heart[87] These cells are present throughout the entire heart, in the following ratio order: right atrium, left atrium, right ventricle, septum, and left ventricle. Isl1 expression is downregulated as soon as the cells adopt a differentiated phenotype, suggesting that this transcription factor delineates a cardiogenic progenitor cell population. In the postnatal heart, Isl1-positive cells are capable of self-renewal and readily differentiate into mature cardiomyocytes after clonal selection. ES cells harboring a reporter gene knock-in in the endogenous Isl1 locus enabled the isolation of Isl1+ cardiac progenitors from mouse and human ES cell systems during in vitro cardiogenesis[88] These cells can also contribute to cardiomyocyte, vascular smooth muscle and endothelial cell lineages when clonally isolated from differentiating ES cells.

Tissue Engineering

Regardless of the type of stem cells used, high-quality transplantation methods must be developed. Tissue engineering is a process by which tissue equivalents are constructed by combining biomaterials with living cells[89–92] Isolated regenerated cardiomyocytes injected into injured hearts have failed to improve cardiac function because they were unable to survive in the recipient heart. Therefore, for cardiac regenerative medicine to be successful, myocardial tissue engineering has emerged as one of the most promising therapeutic methods of stem cell transplantation for patients suffering from severe heart failure.

The challenge in tissue engineering has been the production of functional heart grafts with a 3-dimensional structure[90] To maintain the 3-dimensional structure of tissues, many biomaterials composed of synthetic materials, natural materials and combinations of these are currently being tested[89] In addition to biomaterials, several tissue engineering matrices have been tested. Although the creation of thick cardiac patches has been limited by an inability to supply the high oxygen and energy demands of cardiomyocytes, engineered contractile rings and sheets have been transplanted into small animals successfully and improved cardiac function[93,94] The use of channeled cardiac extracellular matrix (ECM) constructs, oxygen carriers and stacked cardiac sheets to improve thickness has reinforced the direct relationship between perfusion and graft size or cell density[95] We also developed a novel and simple method for making functional myocardial cell sheets that may be used as transplants[96] Polymerized human fibrin-coated dishes are prepared with fibrinogen monomers mixed with thrombin. Cardiomyocytes cultured on these dishes form myocardial cell sheets, which are easily dissociated in an intact state from the polymerized fibrin layer, because the fibrin has been digested by an intrinsic protease. Two overlaid myocardial cell sheets exhibit synchronized spontaneous beating and captured artificial pacing. Transplanted 3-layered myocardial cell sheets exhibit strong spontaneous beating, well-differentiated striations, and an increase in cell size. This simple method of cell-sheet engineering may be applicable for various other cell types.

Vascular tissues and cardiac valves are well-known targets for decellularization and reseeding with endothelial cells, processes involved in creating artificial tissues?[97-100] Recent research revealed the creation of a bioartificial heart.[101] Hearts were decellularized by coronary perfusion with detergents, ensuring that the underlying ECM was preserved, and the constructs were reseeded with cardiac or endothelial cells. Under physiological load and electrical stimulation, constructs could generate pump function in a modified working heart preparation.

Conclusion

Although BM and cardiac stem cells may have a role in cardiac regeneration and have the potential to be used in regenerative medicine, so far they cannot supply adequate amounts of healthy cardiomyocytes for therapeutic purposes. The enormous clinical potential of cardiac regeneration has generated great expectations in both clinicians and patients. Regenerative medicine protocols are already well established and used clinically to treat problems with skin, cartilage, bone, adipose tissue, and corneas. In contrast, cardiac regeneration has to overcome some hurdles before it is clinically viable, including the development of methods to increase the selectivity of cardiomyocyte induction, ensuring enough cardiomyocytes can be produced, and constructing transplantable tissues that include the vascular system. The realization of cardiac regeneration depends on the outcome of basic research and its subsequent application to the clinic. Careful clinical trials using the various stem-cell sources may gradually, but significantly, advance this field, and should be carried out in tandem with further intensive investigations into the basic mechanisms underlying the differentiation process.

References

1. Mudd JO, Kass DA. Tackling heart failure in the twenty-first century. *Nature* 2008; **451:** 919–928.
2. Makino S, Fukuda K, Miyoshi S, Konishi F, Kodama H, Pan J, et al. Cardiomyocytes can be generated from marrow stromal cells in vitro. *J Clin Invest* 1999; **103:** 697–705.
3. Dimmeler S, Zeiher AM, Schneider MD. Unchain my heart: The scientific foundations of cardiac repair. *J Clin Invest* 2005; **115:** 572–583.
4. Fukuda K, Yuasa S. Stem cells as a source of regenerative cardiomyocytes. *Circ Res* 2006; **98:** 1002–1013.
5. Segers VFM, Lee RT. Stem-cell therapy for cardiac disease. *Nature* 2008; **451:** 937–942.
6. Ballard VLT, Edelberg JM. Stem cells and the regeneration of the aging cardiovascular system. *Circ Res* 2007; **100:** 1116–1127.
7. Lipinski MJ, Biondi-Zoccai GGL, Abbate A, Khianey R, Shieban I, Bartunek J, et al. Impact of intracoronary cell therapy on left ventricular function in the setting of acute myocardial infarction: A collaborative systematic review and meta-analysis of controlled clinical trials. *J Am Coll Cardiol* 2007; **50:** 1761–1767.
8. Haider HK, Ashraf M. Bone marrow cell transplantation in clinical perspective. *J Mol Cell Cardiol* 2005; **38:** 225–235.
9. Dimmeler S, Burchfield J, Zeiher AM. Cell-based therapy of myocardial infarction. *Arterioscler Thromb Vasc Biol* 2008; **28:** 208–216.
10. Takahashi K, Yamanaka S. Induction of pluripotent stem cells from mouse embryonic and adult fibroblast cultures by defined factors. *Cell* 2006; **126:** 663–676.
11. Okita K, Ichisaka T, Yamanaka S. Generation of germline-competent induced pluripotent stem cells. *Nature* 2007; **448:** 313–317.
12. Nakagawa M, Koyanagi M, Tanabe K, Takahashi K, Ichisaka T, Aoi T, et al. Generation of induced pluripotent stem cells without Myc from mouse and human fibroblasts. *Nat Biotech* 2008; **26:** 101–106.
13. Takahashi K, Tanabe K, Ohnuki M, Narita M, Ichisaka T, Tomoda K, et al. Induction of pluripotent stem cells from adult human
fibroblasts by defined factors. *Cell* 2007; **131:** 861–872.
14. Park IH, Zhao R, West JA, Yaabuchi A, Huo H, Ince TA, et al. Reprogramming of human somatic cells to pluripotency with defined factors. *Nature* 2008; **451:** 141–146.
15. Yu J, Vodyanik MA, Smuga-Otto K, Antosiewicz-Bourget J, Frane JL, Tian S, et al. Induced pluripotent stem cell lines derived from human somatic cells. *Science* 2007; **318:** 1917–1920.
16. Hanna J, Wernig M, Markoulaki S, Sun CW, Meissner A, Cassady JP, et al. Treatment of sickle cell anemia mouse model with iPS cells generated from autologous skin. *Science* 2007; **318:** 1920–1923.
17. Wernig M, Zhao JP, Pruszak J, Hedlund E, Fu D, Soldner F, et al. Neurons derived from reprogrammed fibroblasts functionally integrate into the fetal brain and improve symptoms of rats with Parkinson's disease. *Proc Natl Acad Sci USA* 2008; **105:** 5856–5861.
18. Evans MJ, Kaufman MH. Establishment in culture of pluripotential cells from mouse embryos. *Nature* 1981; **292:** 154–156.
19. Murry CE, Keller G. Differentiation of embryonic stem cells to clinically relevant populations: Lessons from embryonic development. *Cell* 2008; **132:** 661–680.
20. Manis JP. Knock out, knock in, knock down: Genetically manipulated mice and the Nobel Prize. *N Engl J Med* 2007; **357:** 2426–2429.
21. Klug MG, Soonpaa MH, Koh GY, Field LJ. Genetically selected cardiomyocytes from differentiating embronic stem cells form stable intracardiac grafts. *J Clin Invest* 1996; **98:** 216–224.
22. Kolossov E, Fleischmann BK, Liu Q, Bloch W, Viatchenko-Karpinski S, Manske O, et al. Functional characteristics of ES cell-derived cardiac precursor cells identified by tissue-specific expression of the green fluorescent protein. *J Cell Biol* 1998; **143:** 2045–2056.
23. Thomson JA, Itskovitz-Eldor J, Shapiro SS, Waknitz MA, Swiergiel GG, Marshall VS, et al. Embryonic stem cell lines derived from human blastocysts. *Science* 1998; **282:** 1145–1147.
24. Wakayama T, Tabar V, Rodriguez I, Perry ACF, Studer L, Mombaerts P. Differentiation of embryonic stem cell lines generated from adult somatic cells by nuclear transfer. *Science* 2001; **292:** 740–743.
25. Tabar V, Tomishima M, Panagiotakos G, Wakayama S, Menon J, Chan B, et al. Therapeutic cloning in individual parkinsonian mice. *Nat Med* 2008; **14:** 379–381.
26. Yang X, Smith SL, Tian XC, Lewin HA, Renard JP, Wakayama T. Nuclear reprogramming of cloned embryos and its implications for therapeutic cloning. *Nat Genet* 2007; **39:** 295–302.
27. Doetschman TC, Eistetter H, Katz M, Schmidt W, Kemler R. The in vitro development of blastocyst-derived embryonic stem cell lines: Formation of visceral yolk sac, blood islands and myocardium. *J Embryol Exp Morphol* 1985; **87:** 27–45.
28. Behfar A, Zingman LV, Hodgson DM, Rauzier JM, Kane GC, Terzic A, et al. Stem cell differentiation requires a paracrine pathway in the heart. *FASEB J* 2002; **16:** 1558–1566.
29. Sachinidis A, Fleischmann BK, Kolossov E, Wartenberg M, Sauer H, Hescheler J. Cardiac specific differentiation of mouse embryonic stem cells. *Cardiovasc Res* 2003; **58:** 278–291.
30. Gassanov N, Devost D, Danalache B, Noiseux N, Jankowski M, Zingg HH, et al. Functional activity of the carboxyl-terminally extended oxytocin precursor peptide during cardiac differentiation of embryonic stem cells. *Stem Cells* 2008; **26:** 45–54.
31. Deb A, Davis BH, Guo J, Ni A, Huang J, Zhang Z, et al. SFRP2 regulates cardiomyogenic differentiation by inhibiting a positive transcriptional autofeedback loop of Wnt3a. *Stem Cells* 2008; **26:** 35–44.
32. Takahashi T, Lord B, Schulze PC, Fryer RM, Sarang SS, Gullans SR, et al. Ascorbic acid enhances differentiation of embryonic stem cells into cardiac myocytes. *Circulation* 2003; **107:** 1912–1916.
33. Hakuno D, Takahashi T, Lammerding J, Lee RT. Focal adhesion kinase signaling regulates cardiogenesis of embryonic stem cells. *J Biol Chem* 2005; **280:** 39534–39544.
34. Kanno S, Kim PKM, Sallam K, Lei J, Billiar TR, Shears LL II. Nitric oxide facilitates cardiomyogenesis in mouse embryonic stem cells. *Proc Natl Acad Sci USA* 2004; **101:** 12277–12281.
35. Yutzey KE, Bader D. Diversification of cardiomyogenic cell lineages during early heart development. *Circ Res* 1995; **77:** 216–219.
36. Olson EN. Development: The path to the heart and the road not taken. *Science* 2001; **291:** 2327–2328.
37. Zhang H, Bradley A. Mice deficient for BMP2 are nonviable and have defects in amnion/chorion and cardiac development. *Development* 1996; **122:** 2977–2986.
38. Schultheiss TM, Burch JB, Lassar AB. A role for bone morphogenetic proteins in the induction of cardiac myogenesis. *Genes Dev*

1997; **11:** 451–462.

39. Ladd AN, Yatskievych TA, Antin PB. Regulation of avian cardiac myogenesis by activin/TGF[beta] and bone morphogenetic proteins. *Dev Biol* 1998; **204:** 407–419.

40. Yuasa S, Itabashi Y, Koshimizu U, Tanaka T, Sugimura K, Kinoshita M, et al. Transient inhibition of BMP signaling by Noggin induces cardiomyocyte differentiation of mouse embryonic stem cells. *Nat Biotechnol* 2005; **23:** 607–611.

41. Bejsovec A. Wnt pathway activation: New relations and locations. *Cell* 2005; **120:** 11–14.

42. Veeman MT, Axelrod JD, Moon RT. A second canon: Functions and mechanisms of [beta]-catenin-independent Wnt signaling. *Dev Cell* 2003; **5:** 367–377.

43. Clevers H. Wnt/[beta]-catenin signaling in development and disease. *Cell* 2006; **127:** 469–480.

44. Cadigan KM. Wnt/[beta]-Catenin Signaling: Turning the Switch. *Developmental Cell* 2008; **14:** 322–323.

45. Tzahor E. Wnt/[beta]-catenin signaling and cardiogenesis: Timing does matter. *Dev Cell* 2007; **13:** 10–13.

46. Marvin MJ, Di Rocco G, Gardiner A, Bush SM, Lassar AB. Inhibition of Wnt activity induces heart formation from posterior mesoderm. *Genes Dev* 2001; **15:** 316–327.

47. Schneider VA, Mercola M. Wnt antagonism initiates cardiogenesis in Xenopus laevis. *Genes Dev* 2001; **15:** 304–315.

48. Tzahor E, Lassar AB. Wnt signals from the neural tube block ectopic cardiogenesis. *Genes Dev* 2001; **15:** 255–260.

49. Yamaguchi TP, Takada S, Yoshikawa Y, Wu N, McMahon AP. T (Brachyury) is a direct target of Wnt3a during paraxial mesoderm specification. *Genes Dev* 1999; **13:** 3185–3190.

50. Carol A, Eisenberg LME. WNT11 promotes cardiac tissue formation of early mesoderm. *Dev Dynamics* 1999; **216:** 45–58.

51. Pandur P, Lasche M, Eisenberg LM, Kuhl M. Wnt-11 activation of a non-canonical Wnt signalling pathway is required for cardiogenesis. *Nature* 2002; **418:** 636–641.

52. Nakamura T, Sano M, Songyang Z, Schneider MD. A Wnt- and beta-catenin-dependent pathway for mammalian cardiac myogenesis. *Proc Natl Acad Sci USA* 2003; **100:** 5834–5839.

53. Ueno S, Weidinger G, Osugi T, Kohn AD, Golob JL, Pabon L, et al. From the Cover: Biphasic role for Wnt/beta-catenin signaling in cardiac specification in zebrafish and embryonic stem cells. *Proc Natl Acad Sci USA* 2007; **104:** 9685–9690.

54. Naito AT, Shiojima I, Akazawa H, Hidaka K, Morisaki T, Kikuchi A, et al. Developmental stage-specific biphasic roles of Wnt/beta-catenin signaling in cardiomyogenesis and hematopoiesis. *Proc Natl Acad Sci USA* 2006; **103:** 19812–19817.

55. Lin L, Cui L, Zhou W, Dufort D, Zhang X, Cai CL, et al. beta-Catenin directly regulates Islet1 expression in cardiovascular progenitors and is required for multiple aspects of cardiogenesis. *Proc Natl Acad Sci USA* 2007; **104:** 9313–9318.

56. Klaus A, Saga Y, Taketo MM, Tzahor E, Birchmeier W. Distinct roles of Wnt/beta-catenin and Bmp signaling during early cardiogenesis. *Proc Natl Acad Sci USA* 2007; **104:** 18531–18536.

57. Kehat I, Kenyagin-Karsenti D, Snir M, Segev H, Amit M, Gepstein A, et al. Human embryonic stem cells can differentiate into myocytes with structural and functional properties of cardiomyocytes. *J Clin Invest* 2001; **108:** 407–414.

58. Kehat I, Khimovich L, Caspi O, Gepstein A, Shofti R, Arbel G, et al. Electromechanical integration of cardiomyocytes derived from human embryonic stem cells. *Nat Biotech* 2004; **22:** 1282–1289.

59. Caspi O, Huber I, Kehat I, Habib M, Arbel G, Yankelson L, et al. Transplantation of human embryonic stem cell-derived cardiomyocytes improves myocardial performance in infarcted rat hearts. *J Am Coll Cardiol* 2007; **50:** 1884–1893.

60. Friedenstein AJ, Piatetzky S II, Petrakova KV. Osteogenesis in transplants of bone marrow cells. *J Embryol Exp Morphol* 1966; **16:** 381–390.

61. Blanc KL, Pittenger MF. Mesenchymal stem cells: Progress toward promise. *Cytotherapy* 2005; **7:** 36–45.

62. Pittenger MF, Mackay AM, Beck SC, Jaiswal RK, Douglas R, Mosca JD, et al. Multilineage potential of adult human mesenchymal stem cells. *Science* 1999; **284:** 143–147.

63. Prockop DJ. Marrow stromal cells as stem cells for nonhematopoietic tissues. *Science* 1997; **276:** 71–74.

64. Rickard DJ, Sullivan TA, Shenker BJ, Leboy PS, Kazhdan I. Induction of rapid osteoblast differentiation in rat bone marrow stromal cell cultures by dexamethasone and BMP-2. *Dev Biol* 1994; **161:** 218–228.

65. Osawa M, Hanada K, Hamada H, Nakauchi H. Long-term lymphohematopoietic reconstitution by a single CD34-low/negative hematopoietic stem cell. *Science* 1996; **273:** 242–245.

66. Goodell MA, Rosenzweig M, Kim H, Marks DF, DeMaria M, Paradis G, et al. Dye efflux studies suggest that hematopoietic stem cells expressing low or undetectable levels of CD34 antigen exist in multiple species. *Nat Med* 1997; **3:** 1337–1345.

67. Matsuzaki Y, Kinjo K. Mulligan RC, Okano H. Unexpectedly efficient homing capacity of purified murine hematopoietic stem cells. *Immunity* 2004; **20:** 87–93.

68. Takahashi T, Kalka C, Masuda H, Chen D, Silver M, Kearney M, et al. Ischemia- and cytokine-induced mobilization of bone marrow-derived endothelial progenitor cells for neovascularization. *Nat Med* 1999; **5:** 434–438.

69. Phinney DG, Prockop DJ. Concise Review: Mesenchymal stem/multipotent stromal cells: The state of transdifferentiation and modes of tissue repair current views. *Stem Cells* 2007; **25:** 2896–2902.

70. Docheva D, Popov C, Mutschler W, Schieker M. Human mesenchymal stem cells in contact with their environment: Surface characteristics and the integrin system. *J Cell Mol Med* 2007; **11:** 21–38.

71. Beltrami AP, Urbanek K, Kajstura J, Yan SM, Finato N, Bussani R, et al. Evidence that human cardiac myocytes divide after myocardial infarction. *N Engl J Med* 2001; **344:** 1750–1757.

72. Orlic D, Kajstura J, Chimenti S, Jakoniuk I, Anderson SM, Li B, et al. Bone marrow cells regenerate infarcted myocardium. *Nature* 2001; **410:** 701–705.

73. Quaini F, Urbanek K, Beltrami AP, Finato N, Beltrami CA, Nadal-Ginard B, et al. Chimerism of the transplanted heart. *N Engl J Med* 2002; **346:** 5–15.

74. Deb A, Wang S, Skelding KA, Miller D, Simper D, Caplice NM. Bone marrow-derived cardiomyocytes are present in adult human heart: A study of gender-mismatched bone marrow transplantation patients. *Circulation* 2003; **107:** 1247–1249.

75. Wagers AJ, Sherwood RI, Christensen JL, Weissman IL. Little evidence for developmental plasticity of adult hematopoietic stem cells. *Science* 2002; **297:** 2256–2259.

76. Balsam LB, Wagers AJ, Christensen JL, Kofidis T, Weissman IL, Robbins RC. Haematopoietic stem cells adopt mature haematopoietic fates in ischaemic myocardium. *Nature* 2004; **428:** 668–673.

77. Murry CE, Soonpaa MH, Reinecke H, Nakajima H, Nakajima HO, Rubart M, et al. Haematopoietic stem cells do not transdifferentiate into cardiac myocytes in myocardial infarcts. *Nature* 2004; **428:** 664–668.

78. Kawada H, Fujita J, Kinjo K, Matsuzaki Y, Tsuma M, Miyatake H, et al. Nonhematopoietic mesenchymal stem cells can be mobilized and differentiate into cardiomyocytes after myocardial infarction. *Blood* 2004; **104:** 3581–3587.

79. Strauer BE, Brehm M, Zeus T, Köstering M, Hernandez A, Sorg RV, et al. Repair of infarcted myocardium by autologous intracoronary mononuclear bone marrow cell transplantation in humans. *Circulation* 2002; **106:** 1913–1918.

80. Assmus B, Schachinger V, Teupe C, Britten M, Lehmann R, Döbert N, et al. Transplantation of progenitor cells and regeneration enhancement in acute myocardial infarction (TOPCARE-AMI). *Circulation* 2002; **106:** 3009–3017.

81. Wollert KC, Meyer GP, Lotz J, Ringes-Lichtenberg S, Lippolt P, Briedenbach C, et al. Intracoronary autologous bone-marrow cell transfer after myocardial infarction: The BOOST randomised controlled clinical trial. *Lancet* 2004; **364:** 141–148.

82. Schachinger V, Erbs S, Elsasser A, Haberbosch W, Hambrecht R, Hölschermann H, et al. Intracoronary bone marrow-derived progenitor cells in acute myocardial infarction. *N Engl J Med* 2006; **355:** 1210–1221.

83. Beltrami AP, Barlucchi L, Torella D, Baker M, Limana F, Chimenti S, et al. Adult cardiac stem cells are multipotent and support myocardial regeneration. *Cell* 2003; **114:** 763–776.

84. Oh H, Bradfute SB, Gallardo TD, Nakamura T, Gaussin V, Mishina Y, et al. Cardiac progenitor cells from adult myocardium: Homing, differentiation, and fusion after infarction. *Proc Natl Acad Sci USA* 2003; **100:** 12313–12318.

85. Messina E, De Angelis L, Frati G, Morrone S, Chimenti S, Firodoliso F, et al. Isolation and expansion of adult cardiac stem cells from human and murine heart. *Circ Res* 2004; **95:** 911–921.

86. Tomita Y, Matsumura K, Wakamatsu Y, Matsuzaki Y, Shibuya I, Kawaguchi H, et al. Cardiac neural crest cells contribute to the dormant multipotent stem cell in the mammalian heart. *J Cell Biol* 2005; **170:** 1135–1146.

87. Laugwitz KL, Moretti A, Lam J, Gruber P, Chen Y, Woodard S, et al. Postnatal isl1+ cardioblasts enter fully differentiated cardiomyocyte lineages. *Nature* 2005; **433:** 647–653.

88. Moretti A, Caron L, Nakano A, Lam JT, Bernshausen A, Chen Y, et al. Multipotent embryonic isl1+ progenitor cells lead to cardiac, smooth muscle, and endothelial cell diversification. *Cell* 2006; **127:**

1151 – 1165.

89. Jawad H, Ali NN, Lyon AR, Chen QZ, Harding SE, Boccaccini AR. Myocardial tissue engineering: A review. *J Tissue Eng Regen Med* 2007; **1:** 327 – 342.

90. Masuda S, Shimizu T, Yamato M, Okano T. Cell sheet engineering for heart tissue repair. *Adv Drug Delivery Rev* 2008; **60:** 277 – 285.

91. Christman KL, Lee RJ. Biomaterials for the treatment of myocardial infarction. *J Am Coll Cardiol* 2006; **48:** 907 – 913.

92. Eschenhagen T, Zimmermann WH. Engineering myocardial tissue. *Circ Res* 2005; **97:** 1220 – 1231.

93. Zimmermann WH, Schneiderbanger K, Schubert P, Didie M, Munzel F, Heubach JF, et al. Tissue engineering of a differentiated cardiac muscle construct. *Circ Res* 2002; **90:** 223 – 230.

94. Sekine H, Shimizu T, Yang J, Kobayashi E, Okano T. Pulsatile myocardial tubes fabricated with cell sheet engineering. *Circulation* 2006; **114**(Suppl): I-87 – I-93.

95. Shimizu T, Sekine H, Yang J, Isoi Y, Yamoto M, Kikuchi A, et al. Polysurgery of cell sheet grafts overcomes diffusion limits to produce thick, vascularized myocardial tissues. *FASEB J* 2006; **20:** 708 – 710.

96. Itabashi Y, Miyoshi S, Kawaguchi H, Yuasa S, Tanimoto K, Furuta A, et al. A new method for manufacturing cardiac cell sheets using fibrin-coated dishes and its electrophysiological studies by optical mapping. *Artif Organs* 2005; **29:** 95 – 103.

97. Chen RN, Ho HO, Tsai YT, Sheu MT. Process development of an acellular dermal matrix (ADM) for biomedical applications. *Biomaterials* 2004; **25:** 2679 – 2686.

98. Dellgren G, Eriksson MJ, Brodin LA, Radegran K. Eleven years' experience with the Biocor stentless aortic bioprosthesis: Clinical and hemodynamic follow-up with long-term relative survival rate. *Eur J Cardio-Thorac Surg* 2002; **22:** 912 – 921.

99. Rieder E, Kasimir MT, Silberhumer G, Seebacher C, Wolner E, Simon P, et al. Decellularization protocols of porcine heart valves differ importantly in efficiency of cell removal and susceptibility of the matrix to recellularization with human vascular cells. *J Thorac Cardiovasc Surg* 2004; **127:** 399 – 405.

100. Ketchedjian A, Jones AL, Krueger P, Robinson E, Crouch K, Wolfinbarger L Jr, et al. Recellularization of decellularized allograft scaffolds in ovine great vessel reconstructions. *Ann Thorac Surg* 2005; **79:** 888 – 896.

101. Ott HC, Matthiesen TS, Goh SK, Black LD, Kren SM, Netoff TI, et al. Perfusion-decellularized matrix: Using nature's platform to engineer a bioartificial heart. *Nat Med* 2008; **14:** 213 – 221.

Role of the hinge region of glucocorticoid receptor for HEXIM1-mediated transcriptional repression

Noritada Yoshikawa [a,b,1], Noriaki Shimizu [a,1], Motoaki Sano [c], Kei Ohnuma [a,b], Satoshi Iwata [a], Osamu Hosono [a,b], Keiichi Fukuda [c], Chikao Morimoto [a,b], Hirotoshi Tanaka [a,b,*]

[a] Division of Clinical Immunology, Advanced Clinical Research Center, Institute of Medical Science, University of Tokyo, 4-6-1, Shirokanedai Minato-ku, Tokyo 108-8639, Japan
[b] Department of Rheumatology and Allergy, Research Hospital, Institute of Medical Science, University of Tokyo, Japan
[c] Department of Regenerative Medicine, Keio University School of Medicine, Tokyo, Japan

ABSTRACT

We previously reported that HEXIM1 (hexamethylene bisacetamide-inducible protein 1), which suppresses transcription elongation via sequestration of positive transcription elongation factor b (P-TEFb) using 7SK RNA as a scaffold, directly associates with glucocorticoid receptor (GR) to suppress glucocorticoid-inducible gene activation. Here, we revealed that the hinge region of GR is essential for its interaction with HEXIM1, and that oxosteroid receptors including GR show sequence homology in their hinge region and interact with HEXIM1, whereas the other members of nuclear receptors do not. We also showed that HEXIM1 suppresses GR-mediated transcription in two ways: sequestration of P-TEFb by HEXIM1 and direct interaction between GR and HEXIM1. In contrast, peroxisome proliferator-activated receptor γ-dependent gene expression is negatively modulated by HEXIM1 solely via sequestration of P-TEFb. We, therefore, conclude that HEXIM1 may act as a gene-selective transcriptional regulator via direct interaction with certain transcriptional regulators including GR and contribute to fine-tuning of, for example, glucocorticoid-mediated biological responses.

© 2008 Published by Elsevier Inc.

Glucocorticoid hormone is essential for maintenance of homeostasis and its actions are believed to exclusively be mediated via binding to its cognate receptor glucocorticoid receptor (GR) [1]. The GR is a ligand-dependent transcription factor belonging to the nuclear receptor superfamily. In particular, the GR, mineralocorticoid receptor (MR), androgen receptor (AR), and progesterone receptor (PR), sharing a common structure, compose subfamily NR3C, and are also called oxosteroid receptors because their cognate ligands have C3-ketone group in the steroid A-ring [2]. GR-mediated transcriptional regulation is originally proposed to be mediated via binding of GR to the glucocorticoid response elements (GRE) on the target gene promoters, however, currently considered to be controlled by communication with a variety of cellular factors [3,4]. The GR protein consists of six distinct domains. The N-terminal A/B domains include transactivational function domain 1 (AF-1). The central C-domain constitutes the DNA-binding domain (DBD). The C-terminal E/F-domains contains the ligand-binding domain (LBD) and transactivational function domain 2 (AF-2). The D-domain, which is called hinge region as well, is relatively less conserved across

nuclear receptors, and, concerning GR, was initially suggested to be a flexible linker between the DBD and the LBD, allowing proper DNA binding, dimerization, and nuclear translocation of the receptor [5]. Although several reports have raised the possibility that this hinge region mediates the interaction with a certain classes of nuclear proteins [6,7], its precise role in functional regulation of GR remains unknown.

Transcription is a complex process controlled at various steps, such as initiation, elongation, and termination [8]. Recently, it has become evident that the positive transcription elongation factor b (P-TEFb), which is composed of cyclin-dependent kinase 9 (CDK9) and cyclin T1 (CycT1), stimulates transcription elongation via phosphorylating the C-terminal domain of RNA polymerase II [9]. A nuclear protein HEXIM1 (hexamethylene bisacetamide-inducible protein 1) negatively regulates this transcription elongation via sequestration of P-TEFb using 7SK small nuclear RNA as a scaffold [10]. HEXIM1 consists of an N-terminal self-inhibitory domain, a C-terminal inhibitory domain, and a central basic region (BR) conveying nuclear localization signal (NLS) and 7SK-binding domain [10]. On the other hand, a growing body of evidence indicates that HEXIM1 has other functions for modulation of gene expression. For example, HEXIM1 has been shown to directly bind and modulate the activities of transcription factors including ERα [11], GR [12], and CCAAT/enhancer-binding protein α (C/EBPα [13].

* Corresponding author. Address: Division of Clinical Immunology, Advanced Clinical Research Center, Institute of Medical Science, University of Tokyo, 4-6-1, Shirokanedai Minato-ku, Tokyo 108-8639, Japan. Fax: +81 3 5449 5547.
E-mail address: hirotnk@ims.u-tokyo.ac.jp (H. Tanaka).
[1] These authors equally contributed to this work.

We previously showed that GR binds to the BR of HEXIM1 to form a separate complex distinct from the HEXIM1/7SK/P-TEFb complex [12]. Moreover, overexpression of HEXIM1 decreases ligand-dependent association between GR and a coactivator transcription intermediate factor-2 (TIF2), resulting in suppression of glucocorticoid-responsive gene activation [12]. Since GR inhibition by HEXIM1 was still preserved even after antisense-mediated knockdown of 7SK, we speculated that HEXIM1 could directly suppress GR-mediated transactivation independent of inhibition of transcription elongation [12]. In the present study, we studied molecular details of this GR-HEXIM1 interaction and revealed that the hinge region of GR is responsible for the interaction with HEXIM1. Moreover, we indicated that HEXIM1 BR differentially modulates two distinct gene regulatory pathways: P-TEFb-dependent transcription elongation and suppression of GR-mediated transactivation via direct binding to the hinge region of the receptor.

Materials and methods

Reagents, antibodies, and cells. Dexamethasone (DEX) and troglitazone (TGZ) were purchased from Sigma. Other reagents were from Nacalai Tesque (Kyoto, Japan) unless otherwise specified. Anti-CDK9 antibody was obtained from Santa Cruz Biotechnology. COS-7 and HeLa cells were obtained from RIKEN Cell Bank (Tsukuba, Japan) and cultured in Dulbecco's modified Eagle's medium (Invitrogen) supplemented with 10% fetal calf serum and antibiotics in a humidified atmosphere at 37 °C with 5% CO_2.

Recombinant DNA. cDNAs of human MR, retinoic acid receptor α (RARα), retinoid X receptor α (RXRα), AR, peroxisome proliferator-activated receptor γ (PPARγ), vitamin D receptor (VDR), and farnesoid X-activated receptor (FXR) were kindly gifted from Drs. R.M. Evans (the Salk Institute, La Jolla, CA), H. Nawata (Kyushu University, Fukuoka, Japan), E.A. Jansson (Karolinska Institutet, Stockholm, Sweden), K. Umesono (Kyoto University, Kyoto, Japan), and D.J. Mangelsdorf (University of Texas, Dallas, TX), respectively. The expression plasmids for human wild-type and various truncated GR and other nuclear receptors were generated by cloning appropriate PCR fragments into pCMX-HA vector as described before [14]. The expression plasmids for the wild-type and BR mutated FLAG-HEXIM1 and glutathione-S-transferase (GST)-fused HEXIM1 were generous gifts from Dr. Q. Zhou (UC Berkeley, CA) and described previously [12]. To construct expression plasmids for deletion mutant of the hinge region of GR (488–520 and 491–515a.a.) and PPARγ (173–288a.a.) (pCMX-HA-GRdD1, pCMX-HA-GRdD2, and pCMX-HA-PPARγdD, respectively), cDNAs encompassing the deleted regions with appropriate flanking sequences containing XhoI cloning site were amplified with PCR and subcloned into pCMX-HA-GR and pCMX-HA-PPARγ. To construct the chimeric protein expression plasmids pCMX-HA-GRdD1 + MRD, pCMX-HA-GRdD1 + PPARγD, and pCMX-HA-PPARγdD + GRD, we opened pCMX-HA-GRdD1 and pCMX-HA-PPARγdD at XhoI site, and the cDNA fragments encompassing the hinge region of MR (670–704a.a.), PPARγ (173–288a.a.), and GR (488–520a.a.) were subcloned, respectively. The GRE- and PPAR-response element (PPARRE)-driven reporter plasmids p2xGRE-LUC and p3xPPARRE-LUC, respectively, were described previously [12] and gifted from Dr. E.A. Jansson, respectively.

In vitro protein–protein interaction studies. To obtain the proteins of each nuclear receptor, in vitro transcription and translation was performed using various pCMX-HA plasmids as template with the TNT Coupled Reticulocyte Lysate System (Promega) in the presence of [^{35}S] Met (1000 Ci/mmol, Amersham Biosciences). Ten microliters of each protein was added to HEXIM1-immobilized FLAG-affinity resin or GST- or GST-HEXIM1-immobilized glutathione Sepharose beads and incubated in binding buffer (25 mM Tris–HCl, pH 7.9, 1 mM DTT, 50 mM NaCl, 1 mM PMSF, and 0.1% (v/v) NP-40) at room temperature for 90 min. Then, the beads were washed, and bound proteins were eluted with 1 M NaCl, analyzed on SDS-polyacrylamide gel electrophoresis (SDS–PAGE), and followed by fluorography.

Sequence alignment. Pretty in SeqWeb package (Genetics Computer Group, Accelrys Inc.) was used with default parameters to align the hinge region sequences of GR to that of the other members of the nuclear receptors.

FLAG-affinity purification. Whole cell extracts were prepared from various FLAG-tagged HEXIM1 expressing HeLa cells, applied to Anti-FLAG M2-agarose beads (Sigma-Aldrich), and incubated for 2 h at room temperature. The beads were washed and bound proteins were eluted with SDS-sample loading buffer, and subjected to Western blot analysis using appropriate antibodies.

Transfection and reporter gene assay. Cells were cultured on 6-cm diameter culture dishes and cell culture medium was replaced with OPTI-MEM medium lacking phenol red (Invitrogen) before transfection. Total amount of the plasmids was kept constant by adding appropriate empty vectors and transfection was performed with TransIT-LT1 (Takara). After 6 h of incubation, media were replaced with fresh OPTI-MEM, and the cells were further cultured with ligands for 24 h at 37 °C. Whole cell extracts were prepared and luciferase enzyme activities were determined using Luciferase Assay System (Promega). Relative light units were normalized to the protein amounts determined with BCA Protein Assay Reagent (PIERCE).

Results

The hinge region of GR was essential for the interaction between GR and HEXIM1

To address the protein–protein interaction of GR with HEXIM1, we investigated which region of GR is essential for the interaction with HEXIM1. We synthesized various [^{35}S] Met-labeled GR mutants in vitro (Fig. 1), and applied them onto FLAG-affinity resin bound FLAG-tagged HEXIM1. Since, we preliminarily showed that neither AF-1 nor DBD is prerequisite for the interaction [12], we focused on the relatively C-terminal part of GR including the hinge region and the LBD/AF-2 (D, E, and F domain). As shown in Fig. 1, HEXIM1 bound to not only wild-type GR but also GR 417–777, 487–777, 417–750, 417–640, and 417–520. However, GR 1–489, 1–417, 520–777, and 417–487 did not bind to HEXIM1. These results indicated that the amino acids spanning 487–520, which overlaps with the hinge region, are important for binding to HEXIM1.

Oxosteroid receptors showed amino acid sequence homology in their hinge regions and bound to HEXIM1 in vitro

Among nuclear receptors, amino acid sequence homology of the hinge region was hardly seen except for the oxosteroid receptor subfamily including GR, MR, AR, and PR (Fig. 2A). Given this, we tested whether the representative members of the nuclear receptor superfamily interact with HEXIM1. For that purpose, GST-fused HEXIM1-immobilized beads were incubated with in vitro translated nuclear receptors as indicated in Fig. 2B. As expected, HEXIM1 significantly bound to not only GR but also MR and AR, but to neither PPARγ, RARα, RXRα, VDR, nor FXR (Fig. 2B). To further examine the role of the hinge region for the interaction between GR and HEXIM1, we applied domain deletion and swap analyses (Fig. 2C). Deletion of the hinge region (amino acids 488–520 and 491–515) from GR (GRdD1 and GRdD2, respectively) lost the ability of GR to bind to HEXIM1. GRdD1 + MRD, in which the GR hinge
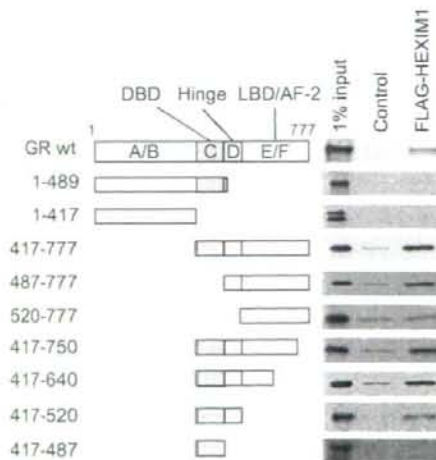

Fig. 1. HEXIM1 interacts with the hinge region of GR. Primary structures of the wild-type and mutant GR are schematically illustrated on the *left*. Numbers depict the positions of amino acids and boxes show the domain structures. FLAG-fused HEXIM1-immobilized beads were incubated with in vitro translated [^{35}S]Met-labeled GRs, bound proteins were analyzed on SDS–PAGE followed by fluorography, and representative results are shown.

A

```
hGR486-521  --M LEARKTKK--KIK IC -ATT VSQETSE P  KTIV
hMR669-705  --- L ARKSKKL KLK I E-EQP    PPPPPPPP SPE
hAR622-662  A MTL ARKLKKL  LKL EE EASSTTSPTEETT KLTVS
hPR633-670  ---VL  RKFKKF KVRVVRALDAVALP PV VP ES ALS
```
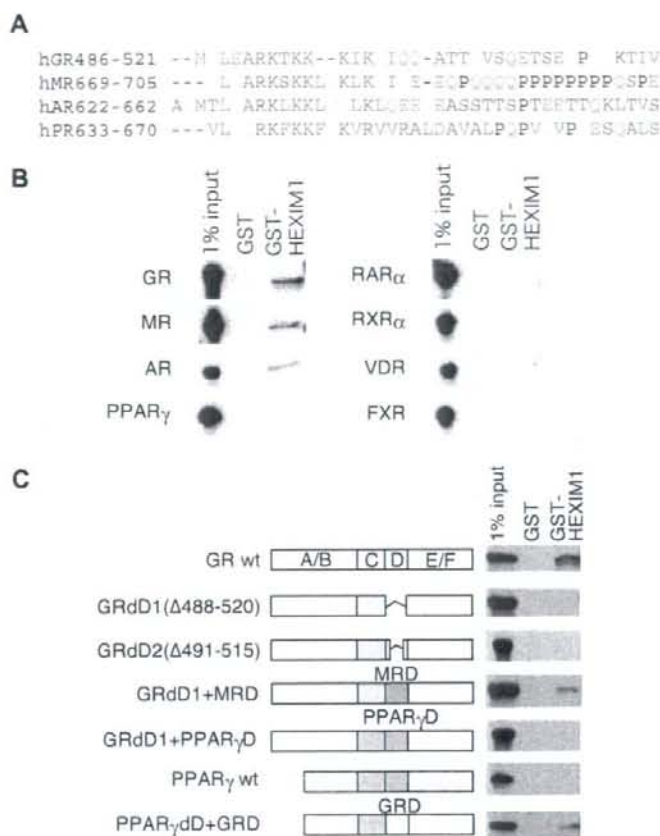
B

C

Fig. 2. The structure of the hinge region of the nuclear receptors determines their binding ability to HEXIM1. (A) Pretty in SeqWeb package (Accelrys Inc.) was used with default parameters to align the hinge sequence of GR to those of the all other members of the nuclear receptors. Homology was not significantly detected except for MR, AR, and PR and the multiple alignments of their hinge regions are shown. Dashes represent gaps in the alignment. (B,C) GST or GST-fused HEXIM1-immobilized beads were incubated with in vitro translated [^{35}S]Met-labeled proteins as indicated, bound receptors were analyzed on SDS–PAGE followed by fluorography, and representative results are shown. Deletion and swap mutants of the hinge region of GR, MR, and PPARγ are schematically shown on the *left* (C). D, D-domain (hinge region); MRD, PPARγD, and GRD depict the D-domain of MR, PPARγ, and GR, respectively (C).

region was substituted with that of MR, bound to HEXIM1, whereas GRdD1 + PPARγD, in which the GR hinge region was substituted with that of PPARγ, did not. Although wild-type PPARγ did not bind to HEXIM1, PPARγdD + GRD, in which the PPARγ hinge region was substituted with that of GR, acquired the ability to bind to HEXIM1 (Fig. 2C). Collectively, we concluded that HEXIM1 binds particular members of nuclear hormone receptors, especially oxosteroid receptors including GR, and that the hinge regions of those receptors may be critical for the interaction.

The role of the hinge region of GR for its transactivation function and HEXIM1-mediated suppression

Next, to analyze the role of the hinge region of GR transactivation function and HEXIM1-mediated transcriptional suppression, wild-type and various mutant GR expression plasmids (See Fig. 2) were transfected with HEXIM1 expression plasmids and GRE-luciferase reporter plasmids in COS7 cells (Fig. 3A). As previously reported, wild-type GR-activated reporter gene expression was suppressed by HEXIM1, and the hinge region-deleted mutant

GRdD1 was transcriptionally silent, however, GRdD2 was capable of inducing GRE-dependent transcription albeit weakly compared with wild-type GR (refs [12,15] and Fig. 3A). Of our surprise, DEX-induced transactivation of GRdD2 was also repressed by HEXIM1 (Fig. 3A). Since not only GRdD1 but also GRdD2 lacks interaction ability with HEXIM1, these results suggest that HEXIM1-mediated GR suppression is regulated mainly by direct interaction between GR and HEXIM1, but that, in the absence of that interaction, effect of sequestration of P-TEFb by HEXIM1 becomes evident. On the other hands, GRdD1 + MRD completely preserved HEXIM1-mediated repression as well as sufficient DEX-induced transactivation, as expected from the results in Fig. 2C. In contrast, GRdD1 + PPARγD and PPARγdD + GRD did not even activate GRE- or PPARRE-driven luciferase reporter gene in the presence of DEX or TGZ, respectively (Fig. 3A and B). Together, it is indicated that, although precise mechanisms remain unknown, the integrity of the receptor architecture involving the hinge region is important in transcriptional regulation by nuclear receptor, especially oxosteroid receptors including GR. In addition, the hinge region may be essential for GR-binding-mediated repression by HEXIM1.
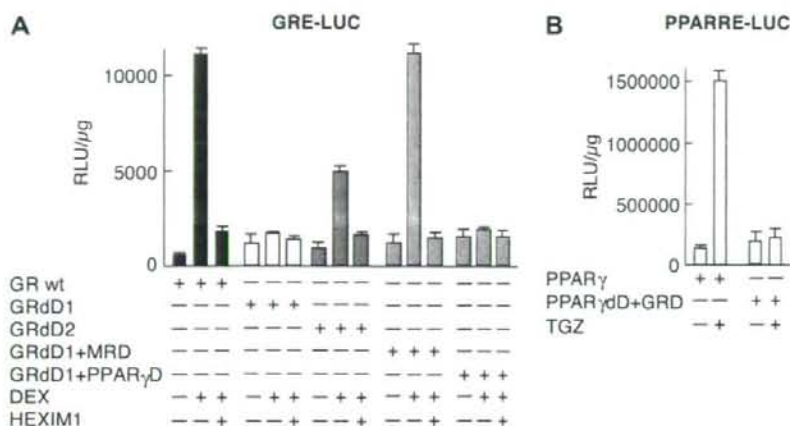
Fig. 3. The requirement of the hinge region of the nuclear receptors for their transactivation function and HEXIM1-mediated repression. (A,B) COS7 cells were cotransfected with 2 μg of reporter plasmids, pGRE-LUC (A) or pPPARRE-LUC (B), and 100 ng each of various receptor expression plasmids (also see Fig. 2C) with or without 500 ng of HEXIM1 expression plasmids as indicated, and further cultured with or without 100 nM DEX (A) or TGZ (B) for 24 h. The cell lysates were prepared for measurement of luciferase activities. All reporter gene experiments were performed in triplicate, results are expressed as relative light units (RLU) per microgram of protein in the extract, and means ± SD are shown.

HEXIM1 mutants lacking P-TEFb-binding ability suppressed GR-mediated but not PPARγ-mediated transactivation

To further analyze the molecular interplay between GR and HEXIM1, we used several HEXIM1 mutants that contain amino acid substitution in distinct portion of BR and differentially affect P-TEFb and GR activity as summarized in Fig. 4A. Those BR mutated HEXIM1 were classified according to the binding ability to P-TEFb, GR, and PPARγ, and tested in GRE- or PPARRE-driven reporter gene assays (Fig. 4B). HEXIM1 dBR + SV, which bound to neither P-TEFb, GR, nor PPARγ, did not affect reporter gene activity of PPARRE-LUC or GRE-LUC (Fig. 4B). Either HEXIM1 mutant, which could bind to GR (GR: + in Fig. 4A), suppressed ligand-dependent activation of GRE-driven reporter gene expression as well as wild-type HEXIM1, irrespective of P-TEFb-binding activity (Fig. 4B, *left panel*). In clear contrast, PPARγ-mediated activation of the reporter gene was repressed solely by wild-type HEXIM1 and 168–177A (P-TEFb: + in Fig. 4A) (Fig. 4B, *right panel*). In these experimental settings, HEXIM1 and its mutants did not affect protein expression of GR or PPARγ (data not shown). It, therefore, is indicated that direct interaction between GR and HEXIM1 plays a major role in HEXIM1-mediated suppression of GR, but that a certain category of the nuclear receptors such as PPARγ is negatively modulated by HEXIM1 solely via sequestration of P-TEFb.

Discussion

We previously revealed that HEXIM1 acts as a negative regulator of GR-mediated transcription, and that HEXIM1-binding to GR does not affect either ligand binding, nuclear translocation, or *in vitro* DNA-binding ability of GR [12]. Here we found that direct association of GR with HEXIM1 requires the hinge region of the receptor and HEXIM1 prefers oxosteroid receptors as an interacting partner among nuclear receptors. Indeed, amino acid sequence of the hinge region is least conserved across nuclear receptors, but the hinge region of GR is homologous only with those of the oxosteroid receptors (Fig. 2A). Although biological function of the very region remains largely unknown, several groups reported the biochemical interaction of the hinge region of GR with coregulatory proteins. For example, a eukaryotic

cochaperone Bag1-M interacts with the hinge region of GR and negatively regulats GR action by inhibition of the ligand and DNA-binding activity of GR [6]. A nuclear receptor COUP-TFII also represses GR-induced transactivation by attracting a corepressor SMRT [7]. Moreover, it is demonstrated that the hinge region contains nuclear retention signal (NRS), overlapping with the NLS in GR [16]. In fact, the substitution of NRS dramatically weakens transactivational ability of GR [16]. We, therefore, cannot completely rule out such possibility that HEXIM1, via interacting with those coregulators or NRS, indirectly represses GR-mediated transcription. However, we previously showed that a certain fraction of HEXIM1 docks in the nucleus with GR [12], and the present study showed that the hinge region of GR is prerequisite for HEXIM1 binding at least *in vitro*. Moreover, our recent chromatin immunoprecipitation assays showed that HEXIM1 suppresses GR recruitment onto the target gene promoter (manuscript in preparation). We, therefore, favor such a model that at least part of HEXIM1 directly binds and sequesters GR to repress transcription initiation triggered by GR. Since it is generally considered that GR coactivators including TIF2 are recruited after GR binding to the promoter [4], this model may fit with our previous observation that overexpression of HEXIM1 decreases ligand-mediated GR-TIF2 association *in situ* [12]. In any case, it should be emphasized that the hinge region and its surrounding architecture may have multiple regulatory roles in GR-mediated signal transduction. The functional differences among GR, GRdD1, and GRdD2 strongly support this idea. Therefore, clarification of the molecular mechanism underlying this multimodal regulation of receptor function would be of importance to understand the integral role of the hinge region of GR.

Originally, it is estimated that majority of nuclear HEXIM1 forms complex with 7SK or Brd4, regulating expression of a large set of class II genes via intervening P-TEFb-mediated elongation reaction [10]. However, our present study rather highlights the distinct role of HEXIM1 independent from inhibition of elongation, gene-selective modulation of transcription. Recently, Montano et al. created mice carrying an insertional mutation in the HEXIM1 gene that disrupted its C-terminal region and found that the HEXIM1 C-terminal region is critical for cardiovascular development [13]. They indicated that HEXIM1 attenuates a repressive effect
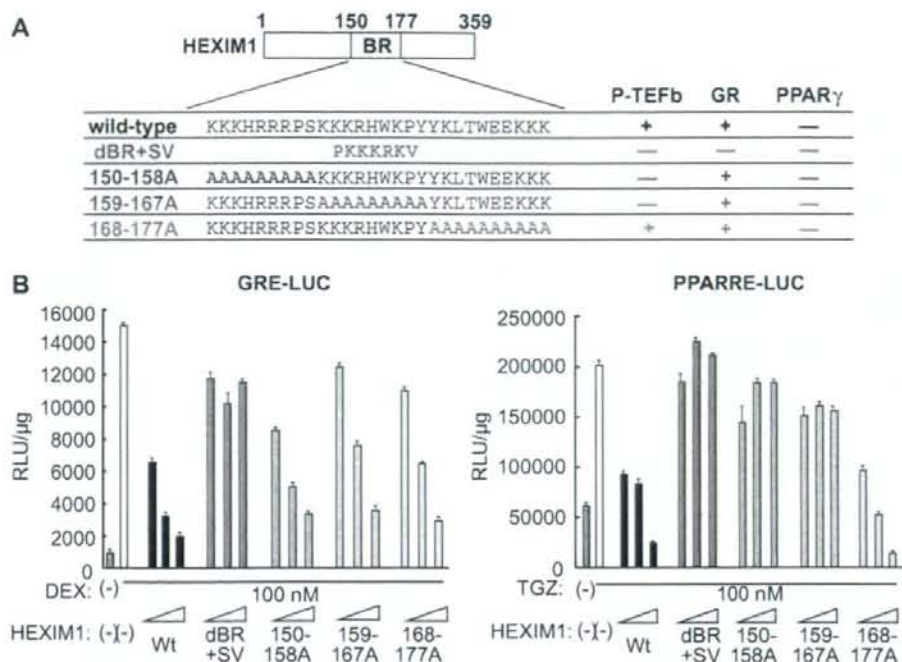
Fig. 4. HEXIM1 represses transactivation function of GR and PPARγ via functionally discrete mechanisms. (A) Primary structure of HEXIM1 (numbers depict amino acid positions), amino acid sequences of HEXIM1 mutants, and their interaction properties with P-TEFb, GR, and PPARγ are summarized. For testing P-TEFb binding, whole cell extracts of FLAG-tagged HEXIM1 or its mutants expressing HeLa cells were prepared and immunoprecipitated with anti-FLAG affinity resin, and CDK9 subunit of P-TEFb was detected using immunoblot. For testing GR and PPARγ binding to HEXIM1 and its BR mutants, various GST-fused HEXIM1-immobilized beads were incubated with in vitro translated [^{35}S]Met-labeled proteins, and bound receptors were analyzed on SDS–PAGE followed by fluorography. (B) COS7 cells were cotransfected with 2 μg each of pGRE-LUC (left) or pPPARRE-LUC (right) and 100 ng of expression plasmids for wild-type GR (left) or PPARγ (right), respectively, with or without increasing amounts (100, 500, and 1000 ng) of expression plasmids for HEXIM1 or its mutants as indicated. The cells were further cultured with or without 100 nM DEX (left) or TGZ (right) for 24 h and the cell lysates were prepared for measurement of luciferase activities. Experiments were performed in triplicate, results are expressed as relative light units (RLU) per microgram of protein in the extract, and means ± SD are shown.

of C/EBPα on vascular endothelial growth factor gene transcription. Note that C-terminal deletion of HEXIM1 does not affect P-TEFb inhibition [13]. Together with our study, it is strongly suggested that HEXIM1 may elicit modulation of gene expression not only via P-TEFb suppression but also via gene context-dependent mechanisms.

At this moment, many questions remain to be answered. It was reported that HEXIM1 represses transactivation function of ERα [11] which belongs to NR3A subfamily of the nuclear receptor superfamily [2]. They showed that HEXIM1 binds with ERα not via the hinge region but via the LBD [11]. Although the requirement of distinct domains for interaction with HEXIM1 between GR and ERα is interesting, we do not know how HEXIM1 can distinguish these two receptors classified in distinct subcategories of the nuclear receptor. This is also the case among oxosteroid receptors, since several members of this receptor group often are simultaneously expressed with fulfilling their own roles in the same tissue [17,18]. Similarly, it is also of particular importance to clarify how HEXIM1, using the central BR, differentially controls P-TEFb inhibition and GR suppression. Further studies, therefore, are clearly needed to address these issues. However, control of GR function *in situ* still remains to be a critical issue in medical fields [19]. Since HEXIM1 has a unique mode of modulation of GR function, HEXIM1 might be a pharmacological target for drug development to modulate GR function.

References

[1] R.M. Sapolsky, L.M. Romero, A.U. Munck, How do glucocorticoids influence stress responses? Integrating permissive, suppressive, stimulatory, and preparative actions, Endocr. Rev. 21 (2000) 55–89.
[2] Nuclear Receptors Nomenclature Committee, A unified nomenclature system for the nuclear receptor superfamily, Cell 97 (1999) 161–163.
[3] T. Rhen, J.A. Cidlowski, Antiinflammatory action of glucocorticoids-new mechanisms for old drugs, N. Engl. J. Med. 353 (2005) 1711–1723.
[4] M.G. Rosenfeld, V.V. Lunyak, C.K. Glass, Sensors and signals: a coactivator/corepressor/epigenetic code for integrating signal-dependent programs of transcriptional response, Genes Dev. 20 (2006) 1405–1428.
[5] R. Kumar, E.B. Thompson, Gene regulation by the glucocorticoid receptor: structure:function relationship, J. Steroid Biochem. Mol. Biol. 94 (2005) 383–394.
[6] M. Kullmann, J. Schneikert, J. Moll, S. Heck, M. Zeiner, U. Gehring, A.C. Cato, RAP46 is a negative regulator of glucocorticoid receptor action and hormone-induced apoptosis, J. Biol. Chem. 273 (1998) 14620–14625.

[7] M.U. De Martino, N. Bhattacharyya , S. Alesci, T. Ichijo, G.P. Chrousos, T. Kino, The glucocorticoid receptor and the orphan nuclear receptor chicken ovalbumin upstream promoter-transcription factor II interact with and mutually affect each other's transcriptional activities: implications for intermediary metabolism, Mol. Endocrinol. 18 (2004) 820–833.

[8] S. Malik, R.G. Roeder, Dynamic regulation of pol II transcription by the mammalian mediator complex, Trends Biochem. Sci. 30 (2005) 256–263.

[9] B.M. Peterlin, D.H. Price, Controlling the elongation phase of transcription with P-TEFb, Mol. Cell 23 (2006) 297–305.

[10] Q. Zhou, J.H. Yik, The Yin and Yang of P-TEFb regulation: implications for human immunodeficiency virus gene expression and global control of cell growth and differentiation, Microbiol. Mol. Biol. Rev. 70 (2006) 646–659.

[11] B.M. Wittmann, K. Fujinaga, H. Deng, N. Ogba, M.M. Montano, The breast cell growth inhibitor, estrogen down regulated gene 1, modulates a novel functional interaction between estrogen receptor alpha and transcriptional elongation factor cyclin T1, Oncogene 24 (2005) 5576–5588.

[12] N. Shimizu, R. Ouchida, N. Yoshikawa, T. Hisada, H. Watanabe, K. Okamoto, M. Kusuhara, H. Handa, C. Morimoto, H. Tanaka, HEXIM1 forms a transcriptionally abortive complex with glucocorticoid receptor without involving 7SK RNA and positive transcription elongation factor b, Proc. Natl. Acad. Sci. USA 102 (2005) 8555–8560.

[13] M.M. Montano, Y.Q. Doughman, H. Deng, L. Chaplin, J. Yang, N. Wang, Q. Zhou, N.L. Ward, M. Watanabe, Mutation of the HEXIM1 gene results in   defects during heart and vascular development partly through downregulation of vascular endothelial growth factor , Circ. Res. (2007).

[14] N. Yoshikawa, K. Yamamoto, N. Shimizu, S. Yamada, C. Morimoto, H. Tanaka, The distinct agonistic properties of the phenylpyrazolosteroid cortivazol reveal interdomain communication within the glucocorticoid receptor, Mol. Endocrinol. 19 (2005) 1110–1124.

[15] S.M. Hollenberg, V. Giguere, P. Segui, R.M. Evans, Colocalization of DNA-binding and transcriptional activation functions in the human glucocorticoid receptor, Cell 49 (1987) 39–46.

[16] A. Carrigan, R.F. Walther, H.A. Salem, D. Wu, E. Atlas, Y.A. Lefebvre, R.J. Hache, An active nuclear retention signal in the glucocorticoid receptor functions as a strong inducer of transcriptional activation, J. Biol. Chem. 282 (2007) 10963–10971.

[17] E.R. de Kloet, R.H. Derijk, O.C. Meijer, Therapy insight: is there an imbalanced response of mineralocorticoid and glucocorticoid receptors in depression?, Nat Clin. Pract. Endocrinol. Metab. 3 (2007) 168–179.

[18] B.R. Walker, Glucocorticoids and cardiovascular disease, Eur. J. Endocrinol. 157 (2007) 545–559.

[19] F. Buttgereit, G.R. Burmester, B.J. Lipworth, Optimised glucocorticoid therapy: the sharpening of an old spear, Lancet 365 (2005) 801–803.

G-CSF Augments Small Vessel and Cell Density in Canine Myocardial Infarciton

Takashi Yagi,[1] Keiichi Fukuda,[2] Jun Fujita,[2] Jin Endo,[1] Yasuyo Hisaka,[2]
Yoshiyuki Suzuki,[3] Masahiko Tamura[4] and Satoshi Ogawa[1]

[1] Cardiopulmonary Division, Department of Internal Medicine, Keio University School of Medicine, Tokyo, Japan
[2] Institute for Advanced Cardiac Therapeutics, Keio University School of Medicine, Tokyo, Japan
[3] Fuji Gotemba Research Labs, Chugai Pharmaceutical Co., Ltd., Shizuoka, Japan
[4] Chugai Research Institute for Medical Science, Inc., Shizuoka, Japan

Abstract: We recently reported that granulocyte-colony stimulating factor (G-CSF) pre-
vented cardiac remodeling by mobilization and differentiation of bone marrow-derived cells
in murine experimental myocardial infarction (MI). Little is known, however, whether these
findings can be reproduced in large animals. The aim of this study is to investigate the effect
of G-CSF after MI in canine model. MI was generated in twenty-six beagle dogs by ligation
of left anterior descending artery. They were divided into two groups: G-CSF group which
received subcutaneous injection of G-CSF (10 µg/kg/day) for 10 days, and the control group
with saline injection. After six weeks, they were subjected to echocardiography and cathe-
terization to measure hemodynamic parameters, and histological analysis was performed.
No dogs died during the period. No hemodynamic changes were observed between these
two groups probably due to the smaller size of the MI than we expected. We found signifi-
cant increase in wall thickness and higher cell density in G-CSF group. Immunohistochemi-
cal staining against α-smooth muscle actin and CD31 revealed increased vessel density
mainly in the epicardium in G-CSF group. The number of survived cardiomyocytes in G-CSF
group was slightly greater than that in the control group, although it was not statistically
significant. These findings suggested G-CSF prevented cardiac remodeling in canine model
not by increasing the cardiomyocytes but by increasing the vessel density and cell numbers
in the infarcted area. (Keio J Med 57 (3) : 139–149, september 2008)

Key words: G-CSF, myocardial infarction, bone marrow derived cell, cardiac remodeling

Introduction

Recent studies have reported that granulocyte-colony
stimulating factor (G-CSF) administration can improve
cardiac function and survival after myocardial infarction
(MI).[1-3] G-CSF can mobilize bone marrow (BM) stem
cells into the systemic circulation, however it remained
unknown whether mobilized-BM cells contribute to the
healing process or prevention of cardiac remodeling after
MI. Experimental and clinical studies have recently sug-
gested that BM cells contribute to the repair of an in-
farcted heart, although the precise mechanism underly-
ing this clinically promising effect remains to be deter-
mined.[4-6] A number of studies have suggested that BM
cells can contribute to regeneration processes in various
tissues.[7,8] Cardiomyocytes derived from BM cells have
been observed both in mice and human,[1,9] and BM-de-
rived cells mobilized by cytokines were capable of re-
generating the myocardial tissue, leading to an improve-
ment in survival and cardiac function after MI.[1] BM
contains both hematopoietic and non-hematopoietic
cells, and the origin of the BM cells with the ability to

Corresponding Author: Keiichi Fukuda, M.D, Ph.D, Institute for Advanced cardiac Therapeutics, Keio University School of Medicine, 35 Shinanomachi,
Shinjuku-ku, Tokyo 160-8582, Japan, Phone: 81-3-5363-3874, Fax: 81-3-5363-3875, E-mail: kfukuda@sc.itc.keio.ac.jp

repair damaged myocardial tissue remained unknown. The identification of specific cell types involved in myocardial repair is a crucial step towards the development of effective stem cell-based therapies for MI. The most likely candidates for the BM-derived stem cells with the ability to regenerate myocardial tissue are hematopoietic stem cells[1,10,11] and mesenchymal stem cells.[12–14] Alvarez-Dolado *et al.* demonstrated that BM-derived cardiomyocytes sporadically detected in non-infarcted mice were exclusively generated by fusion with donor CD45^{+} cells, possibly hematopoietic cells,[15] suggesting that the so-called phenomenon of hematopoietic stem cells 'plasticity' might result from the fusion of hematopoietic stem cells with cells residing in the target tissue. In addition, two recent studies also confirmed that hematopoietic stem cells can not transdifferentiate into cardiomyocytes *in vivo*.[16,17] Another candidates for the regeneration of cardiomyocytes are mesenchymal stem cells; we previously reported that BM mesenchymal stem cells could differentiate into spontaneously beating cardiomyocytes *in vitro*,[12,13] and other groups have repaired the myocardium using mesenchymal stem cells transplantation *in vivo*.[18,19] We recently examined two independent clonal studies to determine the origin of BM-derived cardiomyocytes, and concluded that mesenchymal stem cells had been mobilized and differentiated into cardiomyocytes, but hematopoietic stem cells could not. However, since the number of regenerated cardiomyocytes was only restricted, it is difficult to explain the effect of G-CSF by the cardiomyocyte regeneration.[20]

To further understand the mechanism of beneficial effect of G-CSF, this study is designed to investigate the changes in cellular density and cellular component (endothelial cells, smooth muscle cells, and cardiomyocytes) in the infarcted area of dogs treated with G-CSF administration. We demonstrate that G-CSF treatment increased the number of endothelial cells and myofibroblasts in the infarcted area, which might reinforce the infarcted ventricular wall, and be essential for the improved cardiac function and survival.

Materials and Methods

Animal experiment protocol

All experimental procedures and protocols were reviewed and approved by the Animal Care and Use Committees of the Keio University and conformed to the NIH Guide for the Care and Use of Laboratory Animals. Twenty-three beagle dogs (10 male and 13 female) were anesthetized with pentobarbital (30-35 mg/kg) intravenously, intubated, and the respiration was controlled by a Harvard respirator with a tidal volume of 20 ml/kg/ stroke, the respiratory rate of 10-15 /min, and the room air mixed with 0.5-1 l/min oxygen. The left thoracotomy

was performed at the 4th intercostal space, and the pericardial cradle was prepared. MI was created by ligation of the left anterior descending coronary artery after the first diagonal branch. After ligation, the chest was closed, and the dogs were carefully observed in the recovery room. One day after MI, the dogs were randomly divided into two groups: a control group (n=10) and a G-CSF treated group (n=13). Dogs of G-CSF group were injected subcutaneously with recombinant human G-CSF (10 μg/kg/day), and control group received saline injection subcutaneously for 10 days after MI. The peripheral blood cell counts were examined on the 10th day. Hemodynamic measurement and histological analysis were performed at 6 weeks after MI.

Echocardiographic and hemodynamic analyses

The dogs were similarly anesthetized, mechanically ventilated, and left thoracotomy was performed at the 5th intercostals space. Under direct observation, echocardiography was performed using a Power Vision SSA-380A (Toshiba Medical) equipped with a 2.5 MHz transducer (PSK-25AT, Toshiba Medical). Left ventricular end-diastolic diameter (LVEDD), left ventricular end-systolic diameter (LVESD) and heart rate (HR) were measured by M-mode echocardiography. Fractional shortening (FS) and ejection fraction (EF) were calculated from the following formula: FS=(LVEDD-LVESD)/ LVEDD and EF=(LVEDD^3-LVESD^3) /LVEDD^3. The measurement was performed three times and the mean value was used.

Thereafter, 7 Fr. double micro-tip catheter transducer (model SPC-771, Millar) was inserted from the left femoral artery to the left ventricle (LV), and LV systolic pressure (LVSP), LV end diastolic pressure (LVEDP), LVdP/dt, and -LVdP/dt were measured. Systolic arterial blood pressure (SBP), diastolic arterial blood pressure (DBP) and heart rate (HR) were also measured. Swan-Ganz thermo-dilution catheter was inserted from right femoral vein to pulmonary artery, and pulmonary artery pressure (PAP) and cardiac output (CO) were measured by thermo-dilution method. All the hemodynamic data was measured at three times and the mean value was used.

Histological analysis

After hemodynamic measurements, dogs were sacrificed by rapid intravenous injection of KCl. The hearts were quickly removed. Right ventricle was eliminated, and left ventricle was cut into five transverse slices. LV diameter, infarcted wall thickness were measured at the level of papillary muscles. The percentage of infracted area was calculated by following formula: infracted area (%)=($\sum$[(outer arc length of infarcted myocardium + in-

ner arc length of infracted myocardium)/(outer circle length of whole LV slice + inner circle length of whole LC slice)x(observed LV slice weight)]/(whole LV weight). The infarcted myocardium were sampled from the slice of papillary muscle level and fixed with peri-odate-lysine-paraformaldehyde (PLP) fixative. The samples were embedded in OCT compound or paraffin. Frozen sections (5 μm thickness) were cut by cryostat, and used for immunostaining. The sections were incubated with primary mouse monoclonal antibodies against α-actinin (SIGMA, 1:800), α-smooth muscle actin (αSM A (SIGMA, 1:5000), and CD31 (DAKO, 1:20) for over-night at 4°C. After rinsing with PBS, secondary antibod-ies labeled with Alexa488 were incubated for 30 min at room temperature. The samples were observed with con-focal laser scanning microscopy (LSM510 ver3.0, Karl Zeiss, Germany). Azan staining was performed on paraf-fin-embedded sections.

Quantiative analysis of the histological samples

Cellular number of the infarcted area was measured by Azan staining or TOTO-3 staining. Red-stained area in the Azan staining was processed by Photoshop Ver7.0, and quantitated by NIH image Ver5.8. The nuclei in the samples were visualized by TOTO-3 staining, and their number was counted by NIH image Ver5.8.

Statistical Analysis

Values are shown as mean±SEM. The significance of differences was evaluated by Welch's t test. The proba-bility level accepted for significance was $p < 0.05$.

Results

No dogs died and were dropped out during experimen-tal period in both G-CSF and control groups. There found no apparent adverse effect of G-CSF administra-tion. Both groups of animals' behavior was normal dur-ing experiment.

Peripheral white blood cell counts

To check the bioactivity of human G-CSF in dogs, we measured peripheral blood cell counts (Fig. 1). At 10 days after MI, the WBC counts were significantly elevat-ed to $5.7 \times 10^4/\mu l$ in the G-CSF group, whereas $1.3 \times 10^4/\mu l$ in the control group. There were no differences between the two groups in the RBC counts, but platelets were sig-nificantly decreased to $2.1 \times 10^5/\mu l$ in G-CSF group than in control group ($3.3 \times 10^5/\mu l$), probably due to well-known side effect of G-CSF.
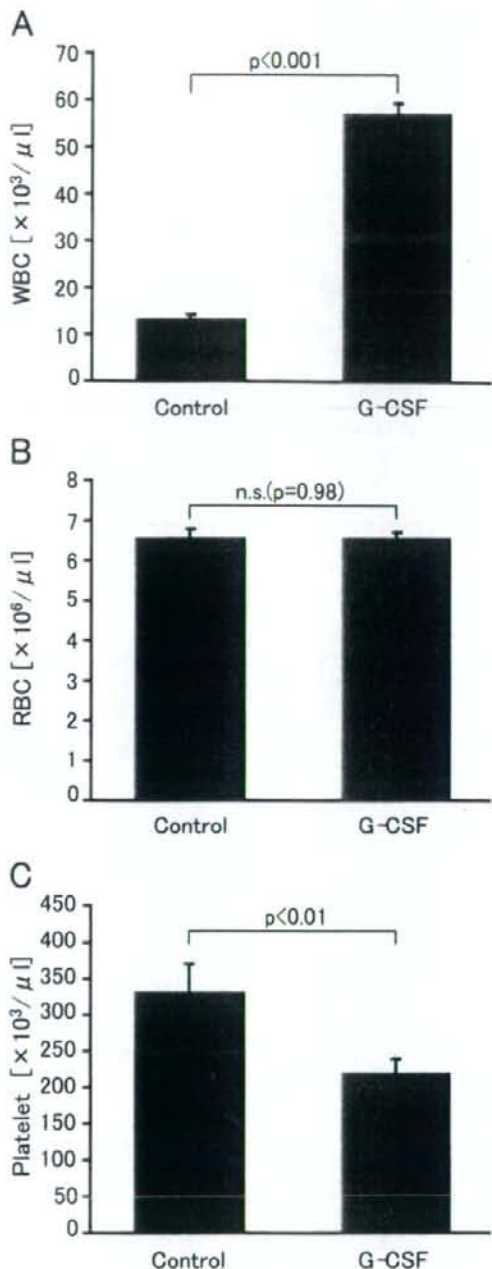

Fig. 1 Effect of G-CSF administration on blood cell counts at 10days.
White blood cell counts (WBC) increased by 4.4-fold of the control, while platelet counts decreased by 0.6-fold. The red cell counts was unchanged.

Table 1 Effects of treatment with G-CSF for 10 days on physiological parameters at 6 weeks after MI in anesthetized dogs

	Sham	Myocardial infarction		P value
		Control	GCSF	
n	4	10	13	
BW (kg)	11.7±0.1	10.1±0.2*	10.6±0.2	0.0875
SBP (mmHg)	118±7	113±5	110±3	0.6634
DBP (mmHg)	95±4	91±4	90±3	0.9047
HR (bpm)	161±12	135±7	146±4	0.1752
LVSP (mmHg)	124±3	108±4*	107±3	0.8894
LVEDP (mmH)	5±1	7±1	5±1	0.2798
LVdP/dt (mmHg/s)	3017±281	2367±237	2329±108	0.8887
-LVdP/dt (mmHg/s)	2996±184	2517±130	2700±134	0.3382
CO (L/min)	1.8±0.1	1.4±0.1*	1.6±0.1	0.3195
PAP (mmHg)	19±1	20±1	18±0	0.1853
pH	7.407±0.010	7.405±0.007	7.394±0.006	0.2334
pCO_2 (mmHg)	35.2±1.6	34.2±0.7	34.9±0.8	0.5053
pO_2 (mmHg)	123.1±4.7	116.4±2.0	115.1±2.2	0.6479
BT (°C)	35.9±0.1	36.5±0.2	36.5±0.1	0.9831

Values are expressed as mean ±SEM. BW: body weight, SBP: systolic arterial blood pressure, DBP: diastolic arterial blood pressure, HR: heart rate, LVSP: left ventricular (LV) systolic pressure, LVEDP: LV end diastolic pressure, LVdP/dt(+) and (-) : maximal and minimal first derivative of LV pressure, CO: cardac output, PAP: mean pulmonary arterial blood pressure, BT: body temperature.

Table 2 Effects of treatment with G-CSF for 10 days on infarct size, cardiac weight, and echocardiographic parameters at 6weeks after MI in anesthetized dogs

	Sham	Myocardial infarction		P value
		Control	G-CSF	
n	4	10	13	
BW (kg)	11.7±0.1	10.1±0.2	10.6±0.2	0.0875
Infarct size	0.012±0.012	0.132±0.011*	0.133±0.009	0.7963
LVW (g)	63.8±3.0	52.6±1.5*	54.5±1.7	0.3988
RVW (g)	21.3±0.6	19.3±0.7	19.6±0.8	0.7965
LVEDD (mm)	21.7±1.9	32.2±0.9*	33.5±0.8	0.2831
LVESD (mm)	12.9±3.1	26.0±0.8*	28.1±0.7	0.0793
HR (bpm)	157±13	138±7	147±4	0.1752
FS	0.42±0.10	0.19±0.02*	0.16±0.02	0.2241
EF	0.71±0.11	0.40±0.03*	0.34±0.03	0.1592

Values are expressed as mean ± SEM. BW: body weight, LVW: left ventricle weight, RVW: right ventricle weight; LVEDD: left ventricular end diastolic dimension, LVESD: left ventricular end systolic dimension, HR: heart rate, FS: fractional shortening, EF: ejection fraction.

Hemodynamic measurements and echocardiogram

Hemodynamic analysis performed at 6 weeks was shown in Table 1. Cardiac output was not significantly different between the control and G-CSF groups. LVEDP seemed to have a tendency to decrease in G-CSF group, but not significant. There was no significant difference between the two groups in other hemodynamic parameters such as body weight, systolic and diastolic blood pressure, LV end-diastolic pressure, pulmonary artery pressure, pH, pCO_2, pO_2, and body temperature.

Echocardiographic measurements were shown in Table 2. There was no significant difference in LV end-diastolic dimension, LV end-systolic dimension, heart rate, fractional shortening and ejection fraction between the two groups. These findings indicated that G-CSF administration did not improve or aggravate the cardiac function after MI.

Macroscopic findings of LV

Anatomical measurement had revealed that there was no difference in LV weight, RV weight and infarcted size between the two groups. Infarct size did not differ between the two groups (Table 2). Fig. 2 revealed the representative photograph of the LV slices at papillary muscle level. Using these LV slices, we investigated LV dimension and infracted wall thickness. There were no significant differences between the groups in LV dimension. However, the infracted wall thickness was significantly greater in G-CSF group, implying that G-SCF might affect the cardiac remodeling after myocardial infarction.

Histological analysis

Since G-CSF can mobilize bone marrow derived cells into peripheral blood, we next investigated the cellular density of the infarcted area. Fig. 3 A-D showed the representative photograph of the azan staining of the infarcted area. Red area indicated the cellular component and blue indicated the interstitial tissue. In both endocardium and epicardium, the red area in the G-CSF treated group seemed to be greater than that of the control group. Quantitative analysis of the red-stained area in both groups was shown in Fig. 3 E,F. The red-stained area of the epicardial layer in G-CSF group was significantly bigger than that of the control group. The red-stained area of the endocardial layer in G-CSF group had a tendency to be bigger than the control group, but it was not statistically significant.

Immunohistochemical analysis

To further investigate the infarcted tissue, we performed immunostaining. Fig. 4 A-D indicated the representative photograph of the nuclear staining with Toto-3. Fig. 4 E,F showed the quantitative analysis of the cell density in the infarcted area. The cell density of both the epicardial and endocardial layer in G-CSF group was significantly higher than those of the control groups. Together with the results of Fig. 3, G-CSF significantly increased the number of cells in the infarcted area.

Fig. 5 A-D showed the representative immunofluorescent microscopy of the infarcted tissue in the control and G-CSF groups with anti-α-SMA antibody. The α-SMA was also expressed in the myofibroblasts in the infarcted area as well as smooth muscle cells. Quantitative analysis of the density of α-SMA-positive cells was shown in Fig. 5 E,F. G-CSF significantly increased the number of α-SMA-positive cells of the epicardial layer and had a tendency to increase that of the epicardial layer in G-CSF group than those in the control groups.

Fig. 6 A-D showed the representative immunofluorescent microscopy of the infarcted area stained with anti-CD31 (PECAM-1) antibody. Quantitative analysis of
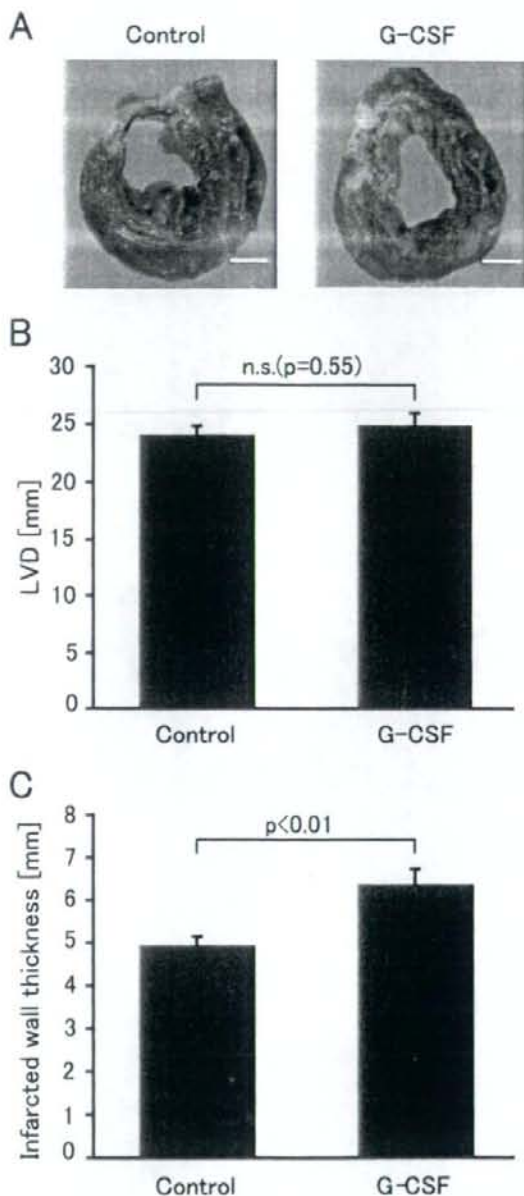

Fig. 2 Effect of G-CSF on left ventricular dimension (LVD) and infarcted wall thickness.

(A) Representative photograph of the slice of infarcted heart at the papillary muscle level in short axis view. Scale bars show 1 cm. (B) LVD of the control and the G-CSF groups was shown. Data were obtained from 10 (Control) and 13 (G-CSF) dogs, respectively. (C) Wall thickness of the infarcted area was shown. Data were obtained from 10 (Control) and 13 (G-CSF) dogs, respectively. Note that wall thickness in G-CSF group was significantly bigger than that of the control group.
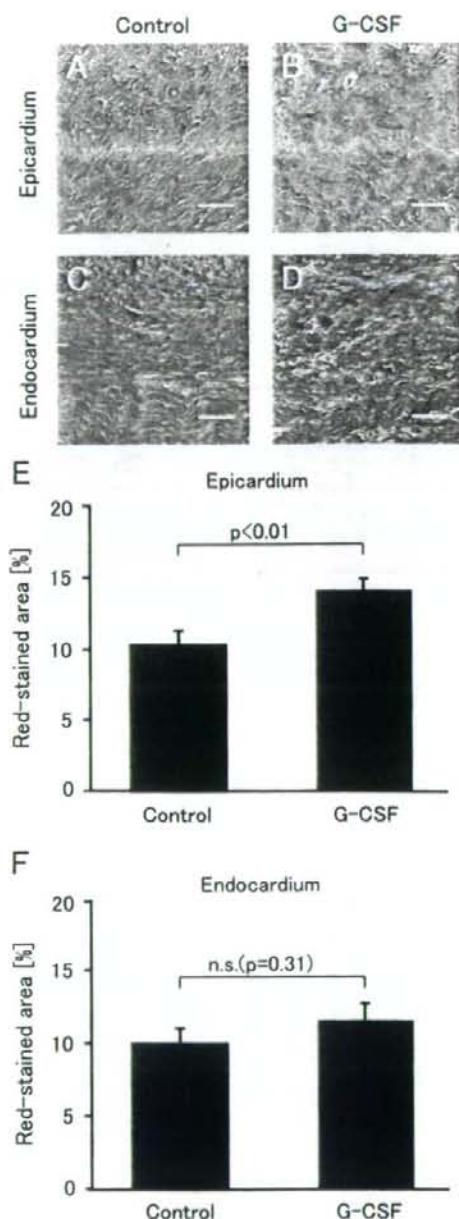
Fig. 3 G-CSF increased the cellular component in the infarcted area

(A-D) Representative microphotograph of the Azan staining of the infarcted area. Blue indicated extracellular matrix and red indicated cellular component. Note that red area was increased by G-CSF administration. Scale bars showed 200 μm. (E, F) Quantative analysis of the red stained area was shown. E and F showed epicardial and endocardial layer, respectively. G-CSF significantly increased the cellular component in the epicardial layer.
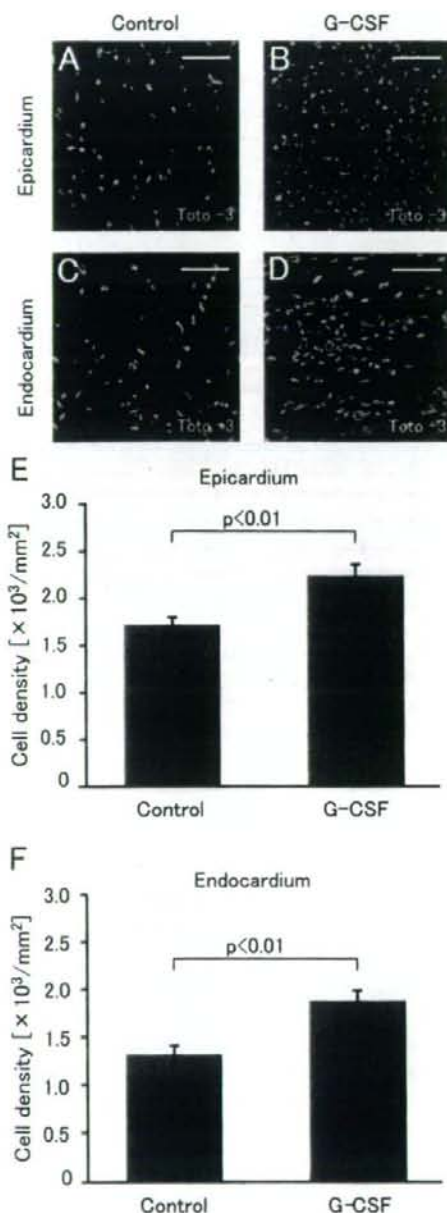
Fig. 4 G-CSF increased the cell number in the infarcted area.

(A-D) Representative microphotograph of the infarcted area by Toto-3, by which nucleus was specifically stained. Scale bars showed 50 μm. (E, F) The cell number in the infarcted area was quatitated. E and F showed epicardial and endocardial layer, respectively. G-CSF significantly increased the cell number in the infarcted area in both epicardial and endocardial layer.
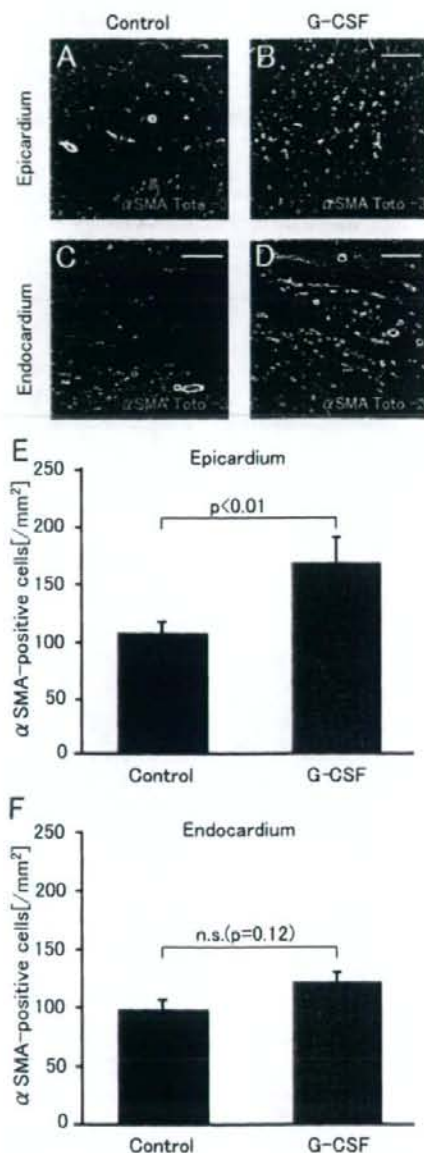
Fig. 5 G-CSF increased the number of α-smooth muscle actin(+) cells in the infarcted area.

(A-D) Epicardial and endocardial layer of the infarced area was separately shown in the control and G-CSF treated groups. Green and blue signals indicated α-smooth muscle actin (α-SMA) (+) and nuclei, respectively. Scale bars show 200μm. (E, F) The number of α-SMA(+) cells of the infarcted area was obtained with immunofluorescent staining, quantiated by NIH image and shown in E and F. Vessel density of the epicardial layer in G-CSF group was significantly higher than that of the control. The number of α-SMA(+) cells of the endocardial layer in G-CSF group has a tendency to be higher than that the control group, but was not statistically significant.

the CD31-positive cell density of the infarcted area was shown in Fig. 6 E,F. G-CSF significantly increased the number of CD31-positive cells of the epicardial layer and had a tendency to increase those of the endocardial layer in G-CSF than those of the control groups. These findings indicated that G-CSF increased the number of endothelial cells, smooth muscle cells and fibroblasts.

Fig. 7 A-D indicated the representative photograph of the infarcted area stained with anti-actinin antibody, and Fig. 7 E,F showed the quantitative analysis. As it is well known, the cardiomyocytes was spared at the subendocardial and subepicardial layer. G-CSF did not significantly affect the survived cardiomyocyte at the epicardial and endocardial layers. G-CSF did not significantly increase the number of cardiomyocytes in the infarcted area. These findings indicated that the survived or regenerated cardiomyocytes were not increased by the administration of G-CSF at the statistically significant level.

Fig. 8 A-D indicated the representative photograph of the infarcted area stained with vimentin antibodies, and Fig. 8 E,F showed the quantitative analysis. G-CSF administration slightly increased the number of vimentin positive cells in the epicardium, although it is not significant. Taken together, these findings indicated that G-CSF administration slightly increased the density of endothelial cells, smooth muscle cells, and fibroblasts in the infarcted area, and its tendency was observed especially at the epicardium.

Discussion

We previously showed that mesenchymal stem cells, not hematopoietic stem cells, could differentiate into cardiomyocytes in vivo after MI.[20] We also reported that bone marrow derived cells can both transdifferentiate into and fuse with cardiomyocytes in pressure overloaded heart using murine pulmonary hypertention and transaortic constriction model.[21] However, the significance of this phenomenon with respect to the G-CSF-induced improvement of cardiac function and survival after MI was not determined. This is due to the fact that the number of regenerated cardiomyocytes was very few even G-CSF was administered, and that it is difficult to explain the beneficial effect of G-CSF to be regenerated cardiomyocytes. Since the fundamental effect of G-CSF was to mobilize the granulocytes and monocytes into peripheral circulation, these cells might infiltrate into the infarcted area.

We recently performed BM transplantation using GFP-transgenic mice as a donor, and investigated the contribution of hematopoietic stem cells -derived cells to the healing process after MI in mice.[22] We found that many hematopoietic stem cell-derived cells, which have a fibroblast-like elongated morphology, are retained at the infarcted myocardium at 7 days post-MI. These cells